

1 **An analysis of the variability of $\delta^{13}\text{C}$ in macroalgae from the Gulf of California: indicative of**
2 **carbon concentration mechanisms and isotope discrimination during carbon assimilation**

3

4 Roberto Velázquez-Ochoa^a, María Julia Ochoa-Izaguirre^b, Martín F. Soto-Jiménez^{c*}

5 ^aPosgrado en Ciencias del Mar y Limnología, Universidad Nacional Autónoma de México, Unidad
6 Académica Mazatlán, Mazatlán, Sinaloa 82040, México

7 ^bFacultad de Ciencias del Mar, Universidad Autónoma de Sinaloa. Paseo Claussen s/n, Mazatlán,
8 Sinaloa 82000, México

9 ^cUnidad Académica Mazatlán, Instituto de Ciencias del Mar y Limnología, Universidad Nacional
10 Autónoma de México (UAM-ICMyL-UNAM), Mazatlán Sinaloa, 82040, México.

11

12 Correspondent author:

13 Telephone number: +52 (669) 9852845 to 48

14 Fax number: +52 (669) 9826133

15 E-mail: martin@ola.icmyl.unam.mx

16

17

18

19 **Abstract**

20 The isotopic composition of carbon in macroalgae ($\delta^{13}\text{C}$) is highly variable, and its prediction is
21 complex concerning terrestrial plants. The determinants of $\delta^{13}\text{C}$ -macroalgal variations were
22 analyzed in a large stock of specimens that vary in taxa and morphology, collected in shallow
23 marine habitats in the Gulf of California (GC) with distinctive environmental conditions. A large
24 $\delta^{13}\text{C}$ variability (-34.6‰ to -2.2‰) was observed. Life forms (taxonomy 57%, morphology and
25 structural organization 34%) explain the variability related to carbon use physiology.
26 Environmental conditions influenced the $\delta^{13}\text{C}$ -macroalgal values but did not change the
27 physiology, which is most likely inherently species-specific. Values of $\delta^{13}\text{C}$ were used as
28 indicators of the presence or absence of carbon concentrating mechanisms (CCMs) and as
29 integrative values of the isotope discrimination during carbon assimilation in the lifecycle
30 macroalgae. Based on $\delta^{13}\text{C}$ signals, macroalgae were classified in three strategies relatives to the
31 capacity of CCM: 1) HCO_3^- uptake ($\delta^{13}\text{C} > -10\text{‰}$), 2) using a mix of CO_2 and HCO_3^- uptake (-
32 $10 < \delta^{13}\text{C} < -30\text{‰}$), and 3) CO_2 diffusive entry ($\delta^{13}\text{C} < -30\text{‰}$). Most species showed a $\delta^{13}\text{C}$ that
33 indicates a CCM using a mix of CO_2 and HCO_3^- uptake. HCO_3^- uptake is also widespread among
34 GC macroalgae, with many Ochrophyta species. Few species belonging to Rhodophyta relied on
35 CO_2 diffusive entry exclusively, while calcifying macroalgae species using HCO_3^- included only
36 *Amphiroa* and *Jania*. The isotopic signature evidenced the activity of CCM, but it was
37 inconclusive about the preferential uptake of HCO_3^- and CO_2 in photosynthesis and the CCM type
38 expressed in macroalgae. In the carbon use strategies study, diverse and species-specific,
39 complementary techniques to the isotopic tools are required.

40 **Keywords:** $\delta^{13}\text{C}$ -macroalgal, carbon-concentrating mechanisms, CO_2 diffusive proxy

41

42 **1. Introduction**

43 Macroalgae show a wide diversity of thallus morphologies (e.g., filamentous, articulated, flattened),
44 structural organization (e.g., surface area/volume ratio), and various photosynthetic pigments (e.g.,
45 Chlorophyll *a*, *b*, phycocyanin) (Lobban and Harrison, 1994). According to the predominant pigment
46 contents in the thallus, macroalgae are classified into three Phyla. The interaction of morphologies
47 and photosynthetic pigments is classified into dozens of groups (Balata et al., 2011; Littler and
48 Littler, 1980; Littler and Arnold, 1982). For example, the mixture of chlorophyll (*a*, *b*) and
49 carotenoids is dominant in Chlorophyta; chlorophyll (*a*, *c*) and fucoxanthin carotenoid is dominant
50 in Ochrophyta, while Rhodophyta contains chlorophyll (*a*, *d*), carotenoid, and a mixture of
51 phycobilin (e.g., phycocyanin, phycoerythrin, allophycocyanin) (Bold and Wynne, 1978; Gateau et
52 al., 2017; Masojidek et al., 2004). Both traits work as an excellent approximation to explain the
53 fundamentals of metabolism, growth, zonation, and colonization (Littler and Littler, 1980; Littler
54 and Arnold, 1982; Nielsen and Sand-Jensen, 1990; Vásquez-Elizondo and Enríquez, 2017).

55 In marine environments, where $\text{pH} \sim 8.1 \pm 1$, the diffusion rate of CO_2 in seawater is low. Thus, HCO_3^-
56 accounts for 98% of the total dissolved inorganic carbon (DIC), resulting in a high $\text{HCO}_3^-:\text{CO}_2$ ratio
57 (150:1) (Sand-Jensen and Gordon, 1984). Low CO_2 concentrations in seawater, which limit
58 macroalgae growth, are compensated by carbon concentrating mechanisms (CCMs) that increase the
59 internal inorganic carbon concentration near the site of RuBisCo activity (Giordano et al., 2005).
60 Therefore, the absorption of HCO_3^- by most macroalgae is the primary source of inorganic carbon
61 for photosynthesis, but some species depend exclusively on the use of dissolved CO_2 that enters cells
62 by diffusion (Beardall and Giordano, 2002; Giordano et al., 2005; Maberly et al., 1992; Raven et al.,
63 2002a, Raven et al., 2002b). Hence, macroalgal species with productivity limited by lacking CCM's
64 (have low plasticity for carbon inorganic forms uptake) seems to be restricted to subtidal habitats
65 and composed mainly by red macroalgae (but without a morphological patron apparent) (Cornwall

66 et al., 2015; Kübler and Dungeon, 2015). The rest of the macroalgae with CCM occupies from the
67 intertidal to the deep subtidal.

68 The habitat features and environmental conditions in marine ecosystems modify the main
69 macroalgae photosynthesis drivers, such as light (Anthony et al., 2004; Johansson and Snoeijs,
70 2002), DIC (Brodeur et al., 2019; Zeebe and Wolf-Gladrow, 2001), and inorganic nutrients (Ochoa-
71 Izaguirre and Soto-Jiménez, 2015; Teichberg et al., 2010). These factors could generate negative
72 consequences for their productivity, principally when they cause resources limitation. Each factor
73 varies from habitat to habitat (e.g., local scale: from intertidal to subtidal and global scale: from
74 temperate to tropical regions), and as in response to these environmental changes, macroalgae can
75 modulate their photosynthetic mechanism (Dudgeon et al., 1990; Kübler and Davison, 1993;
76 Lapointe and Duke, 1984; Young and Beardall, 2005). The modulation, to increase their
77 photosynthetic activity (up-and-down-regulation processes), implies a physiological acclimation
78 enhancing the transport of DIC (CO_2 , HCO_3^-) into the cell and its fixation rates (Enríquez and
79 Rodríguez-Román, 2006; Giordano et al., 2005; Klenell et al., 2004; Madsen and Maberly, 2003;
80 Rautenberger et al., 2015; Zou et al., 2004).

81 The $\delta^{13}\text{C}$ -macroalgal indicates the carbon source used (CO_2 or HCO_3^-) in photosynthesis and allows
82 inferring the presence or absence of CCM's (Giordano et al., 2005; Maberly et al., 1992; Raven et
83 al., 2002a). However, the isotopic signature may be inconclusive for determining the carbon source's
84 preference (Roleda and Hurd, 2012). Also, the $\delta^{13}\text{C}$ signal in the algal thallus can be used to indicate
85 of the physiological state of photosynthetic metabolism (Kim et al., 2014; Kübler and Dungeon,
86 2015). For example, $\delta^{13}\text{C}$ variability depends, in part, on the life forms as taxonomy, morphology,
87 and structural organization (Lovelock et al., 2020; Marconi et al., 2011; Mercado et al., 2009; Roleda
88 and Hurd, 2012). $\delta^{13}\text{C}$ is also modulated by the interaction to environmental conditions (e.g., light,
89 DIC, and nutrients) (Carvalho et al., 2010a; Carvalho et al., 2010b; Cornelisen et al., 2007; Dudley

90 et al., 2010; Mackey et al., 2015; Rautenberger et al., 2015; Roleda and Hurd, 2012). In this study,
91 our objective was to investigate the contributions of life forms, the changes in the habitat features,
92 and environmental conditions to the $\delta^{13}\text{C}$ macroalgal variability in communities in the Gulf of
93 California (GC). We collected a large stock of macroalgae specimens of a diversity of species
94 characterized by various morphological and physiological properties to reach our objective. Besides
95 high diversity, in terms of life forms, we selected various shallow marine habitats along a latitudinal
96 gradient in the GC or the sample collection, characterized by unique and changing environmental
97 factors. The GC features abundant and diverse macroalgae populations, acclimated and adapted to
98 diverse habitats with environmental conditions, determining the light, DIC, and nutrients
99 availability. The $\delta^{13}\text{C}$ signal from the thallus of macroalgae was used as indicative of the presence
100 or absence of CCMs and as integrative values of the isotope discrimination during carbon
101 assimilation and respiration along lifecycle macroalgae in macroalgae communities in the GC in the
102 function of taxa and environmental factors (Díaz-Pulido et al., 2016; Hepburn et al., 2011; Maberly
103 et al., 1992; Raven et al., 2002a). Because the GC is a subtropical zone with high irradiance and
104 specimens were collected in the intertidal and shallow subtidal zone, we expect to find a high
105 proportion of species with active uptake HCO_3^- ($\delta^{13}\text{C} > -10\%$). A third objective was to explore any
106 geographical pattern in the $\delta^{13}\text{C}$ macroalgal along and between the GC bioregions. Previous studies
107 have indicated changes in the $\delta^{13}\text{C}$ signal with latitude, mainly related to the light and temperature
108 (Hofmann and Heesch, 2018; Lovelock et al., 2020; Marconi et al., 2011; Mercado et al., 2009;
109 Stepien, 2015). Macroalgae as biomonitors constitute an efficient tool in monitoring programs in
110 large geographical regions (Balata et al., 2011) and for environmental impact assessments (Ochoa-
111 Izaguirre and Soto-Jiménez, 2015).

112 **2. Materials and Methods**

113 **2.1. Gulf of California description**

114 The Gulf of California is a subtropical, semi-enclosed sea of the Pacific coast of Mexico, with
115 exceptionally high productivity being the most important fishing region for Mexico and one of the
116 most biologically diverse worldwide marine areas (Espinosa-Carreón and Valdez-Holguín 2007;
117 Lluch-Cota et al., 2007; Páez-Osuna et al., 2017; Zeitzschel, 1969). The Gulf of California
118 represents only 0.008% of the area covered by the seas of the planet (265,894 km², 150 km wide,
119 and 1000 km long covering >9 degrees latitude). However, the GC has a high physiographic diversity
120 and is biologically mega-diverse with many endemic species, including ~ 766 macrofauna species
121 and/or sub-species where the major number belong to Arthropoda (118 spp) and Mollusca (460) taxa
122 (Brusca et al., 2005; Espinosa-Carreón and Escobedo-Urías, 2017; Wilkinson et al., 2009) and 116
123 macroalgae species (Espinoza-Avalos, 1993; Norris, 1975, 1985).

124 Regionalization criteria of the GC include phytoplankton distribution (Gilbert and Allen, 1943),
125 topography (Rusnak et al., 1964) and depth (Álvarez-Borrego, 1983), oceanographic characteristics
126 (Álvarez-Borrego, 1983; Marinone and Lavin 2003; Roden and Emilson, 1979), biogeography
127 (Santamaría-del-Ángel et al., 1994), and bio-optical characteristics (Bastidas-Salamanca et al.,
128 2014). The topography is variable along with GC, includes submarine canyons, basins, and variable
129 continental platforms. Besides, GC presents complex hydrodynamic processes, including internal
130 waves, fronts, upwelling, vortices, mixing of tides. The gulf's coastline is divided into three shores:
131 extensive rocky shores, long sandy beaches, numerous scattered estuaries, coastal lagoons, and open
132 muddy bays, tidal flats, and coastal wetlands (Lluch-Cota et al., 2007).

133 The Gulf of California is different in the north and the south, related to a wide range of
134 physicochemical factors. The surface currents seasonally change direction and flow to the southeast

135 with maximum intensity during the winter and to the northwest in summer (Roden, 1958). The
136 northern part is very shallow (<200 m deep averaged), divided into upper Gulf, northern Gulf, and
137 Midriff Islands region (Roden, 1958, Roden and Groves, 1959). The surrounding deserts largely
138 influence this region (Norris, 2010) shows marked seasonal changes in coastal surface seawater
139 temperatures (Marinone, 2007; Martínez-Díaz de León et al., 2006). Tidal currents induce a
140 significant cyclonic circulation through June to September and anticyclonic from November to April
141 (Bray, 1988; Carrillo et al., 2002; Martínez-Díaz-de-León, 2001; Velasco-Fuentes and Marinone,
142 1999). The southern part consists of a series of basins whose depths increase southwards (Fig. 1).
143 The intertidal macroalgae in the southern region are subject to desiccation, mostly during summer.
144 The water column's physicochemical characteristics are highly influenced by the contrasting climatic
145 seasons in the GC, the dry season (nominally from November to May), and the rainy season (from
146 June to October). Annual precipitation ($1,080 \text{ mm y}^{-1}$) and evaporation (56 mm y^{-1}) rates registered
147 during the past 40 years were $881 \pm 365 \text{ mm y}^{-1}$ and $53 \pm 7 \text{ mm y}^{-1}$, respectively (CNA, 2012).

148 In the GC exist around 669 species, including 116 endemic species (Espinoza-Avalos, 1993; Norris,
149 1975; Pedroche and Senties, 2003). Many endemic species currently have a wide distribution along
150 the Pacific Ocean coast, but with GC origin (Aguilar-Rosas et al., 2014; Dreckman, 2002). Based on
151 oceanographic characteristics (Roden and Groves, 1959) and in the endemic species distribution
152 (Aguilar-Rosas and Aguilar-Rosas, 1993; Espinoza-Avalos, 1993), the GC can be classified into
153 three phycofloristic zones: 1) the first zone located from the imaginary line connecting San
154 Francisquito Bay, B.C. to Guaymas, Sonora, with 51 endemic species. 2) the second zone with an
155 imaginary line from La Paz Bay (B.C.S.) to Topolobampo (Sinaloa) with 41 endemic species. 3) the
156 third zone is located with an imaginary line from Cabo San Lucas (B.C.S.) to Cabo Corrientes
157 (Jalisco) with ten endemic species. Besides, 14 endemic species are distributed throughout the GC

158 (Espinoza-Ávalos, 1993). The macroalgal communities are subject to the changing environmental
159 conditions in the diverse habitats in the GC that delimits their zonation, which tolerates a series of
160 anatomical and physiological adaptations to water movement, temperature, sun exposure, and light
161 intensities, low pCO₂, desiccation (Espinoza-Avalos, 1993).

162 **2.1 Macroalgae sampling**

163 In this study, the GC coastline (21°-30°N latitude) was divided into six coastal sectors based on the
164 three phycofloristic zones along peninsular and continental GC coastlines (Fig. 1a). In each coastal
165 sector, selected ecosystems and representative habitats were sampled based on macroalgae
166 communities' presence and habitat characterization. Habitats were classified by substrate type (e.g.,
167 sandy-rock, rocky shore), hydrodynamic (slow to faster water flows), protection level (exposed or
168 protected sites), and immersion level (intertidal or subtidal) (Fig. 1b).

169 Based on the local environmental factors, 4-5 macroalgae specimens of the most representative
170 species were gathered by hand (free diving) during low tide. A total of 809 composite samples were
171 collected from marine habitats along both GC coastlines. The percentages of specimens collected for
172 the substrate type were sandy-rock 28% and rocky shores 72% based on the habitat features. In the
173 hydrodynamic, 30% of the specimens were collected in habitats with slow to moderate and 70% with
174 moderate to fast water movement. Regarding the protection level, 57% were exposed specimens,
175 and 43% were protected. Finally, 56% were intertidal and 44% subtidal macroalgae organisms
176 concerning the emersion level. About half of the protected specimens were collected in isolated rock
177 pools, which was noted.

178 In 4-5 sites of each habitat, we measured *in situ* the salinity, temperature, and pH by using a
179 calibrated multiparameter sonde (Y.S.I. 6600V) and the habitat characteristics mentioned above

180 noted. Besides, composite water samples were collected for a complimentary analysis of nutrients,
181 alkalinity (and their chemical components), and $\delta^{13}\text{C}$ -DIC (data non-included). Briefly, the
182 representative habitats were classified by pH levels in >9.0 “alkalinized”, 7.9 - 8.2 ‘typical’ and <7.9
183 “acidified”. Based on the temperature in colder $<20^\circ\text{C}$, typical 20 - 25°C , and warmer $>25^\circ\text{C}$. 72% of
184 the specimens were collected at typical pH values, 22% alkalinized, and 6% in acidified seawater.
185 Regarding the temperature, about 55% of the specimens were collected at typical, 31% at warmer,
186 and 14% at colder seawaters. Regarding salinity, most of the ecosystems showed typical values for
187 seawater (35.4 ± 0.91 ups, from 34.5 to 36.1 ups). In this study, the collection surveys were conducted
188 during spring (March-April) and dry season (nominally from November to May) from 2008 to 2014.
189 Only in a few selected ecosystems located at C1, C2, and C3 sectors, one sampling survey was
190 conducted at the end of the rainy season (nominally from June to October in 2014). Thus, these
191 ecosystems were possible to include habitat with a salinity range varying from estuarine (23.5 ± 3.0
192 ups) to hypersaline (42.7 ± 7.0 ups) values. These habitats were mainly isolated rock pools, and only
193 a few were sites near tidal channels receiving freshwater discharges. About 95% of the specimens
194 were collected at typical seawater salinity (34-36 ups) and only 1.5 and 3.5% in estuarine (<30 ups)
195 and hypersaline (>37 ups) environments, respectively. Detailed information on the selected shallow
196 marine ecosystems, habitat characterization, and environmental conditions is summarized in the
197 inserted table in Fig. 1.

198 **2.2 Macroalgae processing and analysis of the isotopic composition of carbon**

199 The collected material was washed *in situ* with surface seawater to remove the visible epiphytic
200 organisms, sediments, sand, and debris and then thoroughly rinsed with MilliQ water. The composite
201 samples were double-packed in a plastic bag, labeled with the locality's name and collection date,
202 placed in an ice-cooler box to be kept to 4°C , and immediately transported to the laboratory UAS-

203 Facimar in Mazatlán. In the field, sample aliquots were also preserved in 4% v/v formaldehyde
204 solution for taxonomic identification to the genus or species level (when possible). The following
205 GC macroalgal flora identification manuals were consulted (Abbot and Hollenberg, 1976; Dawson,
206 1944; 1954; 1956; 1961; 1962; 1963; Norris, 2010; Ochoa-Izaguirre et al., 2007; Setchell and
207 Gardner, 1920; 1924).

208 In the laboratory, macroalgae samples were immediately frozen at -30°C until analysis. Then,
209 samples were freeze-dried at -38°C and 40 mm Hg for 3 days, upon which they were ground to a
210 fine powder and exposed to HCl vapor for 4 h (acid-fuming) to remove carbonates and dried at 60°C
211 for 6 h (Harris et al., 2001). Aliquots of ~5 mg were encapsulated in tin cups (5x9 mm) and stored
212 in sample trays until analysis. Macroalgae samples were sent to the Stable Isotope Facility (SIF) at
213 the University of California at Davis, CA, USA. Natural ¹³C relative abundance relative to ¹²C in
214 samples was determined with mass spectrometry, using a Carlo Erba elemental analyzer attached to
215 a Finnigan Delta S mass spectrometer equipped with a Europa Scientific stable isotope analyzer
216 (ANCA-NT 20-20) and a liquid/solid preparation unit (PDZ, Europa, Crewz, UK). Isotope ratios of
217 the samples were calculated using the equation δ (‰) = $(R_{\text{sample}}/R_{\text{standard}} - 1) \times 1000$, where $R = {}^{13}\text{C}/{}^{12}\text{C}$.
218 The R_{standard} is relative to the international V-PDB (Vienna PeeDee Belemnite) standard. During the
219 isotopic analysis, the SIF lab used different certified reference materials (e.g., IAEA-600, USGS-40,
220 USGS-41, USGS-42, USGS-43, USGS-61, USGS-64, and USGS-65) for the analytical control
221 quality. The analytical uncertainties reported for the SIF lab were 0.2‰ for $\delta^{13}\text{C}$
222 (<https://stableisotopefacility.ucdavis.edu/13cand15n.html>). We also included triplicate aliquots of
223 several specimens of the same species and condition, collected from one patch, or attached to the
224 same substrate, to assess the method error by sampling and processing procedural. The
225 methodological uncertainties were <0.4‰.

226 2.3. Analysis of $\delta^{13}\text{C}$ -macroalgal variability

227 The variability of $\delta^{13}\text{C}$ values in macroalgae was analyzed in function of the taxonomy (phylum,
228 genus, and species) and morpho-functional groups (e.g., thallus structure, growth form, branching
229 pattern, and taxonomic affinities; Balata et al., 2011; Ochoa-Izaguirre and Soto-Jiménez, 2015).
230 The carbon fixation strategies in the macroalgae communities of the GC were identified by $\delta^{13}\text{C}$
231 (Díaz-Pulido et al., 2016; Hepburn et al., 2011), in agreement with the Maberly et al. (1992) and
232 Raven et al. (2002a) thresholds. So, macroalgae were classified into three strategies for DIC
233 uptake: 1) CCM-only by active uptake HCO_3^- ($\delta^{13}\text{C} > -10\text{‰}$), 2) CCM active uptake HCO_3^- and
234 diffusive uptake CO_2 ($\delta^{13}\text{C} < -11$ to -30‰), and 3) Non-CCM, CO_2 by diffusion only ($\delta^{13}\text{C} < -30\text{‰}$).
235 The measured $\delta^{13}\text{C}$ -macroalgal signals are integrative of the discrimination by photosynthesis
236 ($\Delta^{13}\text{C}_p$) on the carbon source ($\delta^{13}\text{C}$ -DIC in seawater), respiration ($\Delta^{13}\text{C}_r$), and probable CO_2 leak
237 out inside the cell during the CCM process (Carvalho et al., 2009a; Carvalho et al., 2009b; Raven
238 et al., 2005; Sharkey and Berry, 1985).

239 Macroalgae were grouped according to their morpho-functional characteristics proposed initially by
240 Littler and Littler (1980) and modified by Balata et al. (2011). Most of the macroalgae species
241 showed a limited distribution along the GC coastlines. Few cosmopolites' species included
242 *Colpomenia tuberculata*, *Sargassum sinicola*, *Padina durvillei*, and *Ulva lactuca*. Also, not all
243 morphofunctional groups and taxon were present in every site during each sampling survey, and the
244 sample size in each group varied for taxa, location, and time.

245 A basic statistical analysis of $\delta^{13}\text{C}$ values in different macroalgae groups was applied to distribute
246 and calculate the arithmetic mean, standard deviation, minimum and maximum. Because not all
247 macroalgal species were present in sufficient numbers at different collection habitats, several

248 macroalgal groups were not considered for statistical analysis. We compared taxon and
249 morphofunctional groups collected in the same habitat (within-subjects factor) by multivariate
250 analysis of variance. When differences were noted, a Tukey-Kramer HSD (Honestly Significant
251 Difference) test was performed. Besides, variations of $\delta^{13}\text{C}$ macroalgal in specimens of the same
252 morpho-functional and taxon collected in different habitats were also investigated with a Kruskal-
253 Wallis test.

254 The relationships between $\delta^{13}\text{C}$ with the inherent macroalgae properties (taxon and morphology),
255 biogeographical collection zone (GC coastline and coastal sector), habitat features (substrate,
256 hydrodynamic, protection, and emersion level), and environmental conditions (temperature, pH, and
257 salinity) were examined through simple and multiple linear regression analyses. Excepting
258 temperature, pH, and salinity, most of the independent variables are categorical independent
259 variables. Simple linear regression analyses were performed to establish the relationships between
260 $\delta^{13}\text{C}$ -macroalgal with each environmental parameter analyzed as possible driving factors (e.g.,
261 temperature, salinity, and pH). Multiple linear regression analyses were conducted to evaluate the
262 combined effects of those independent variables (macroalgae properties, biogeographical collection
263 zone, habitat features, and environmental conditions) on the $\delta^{13}\text{C}$ -macroalgal. In the multivariable
264 regression model, the dependent variable, $\delta^{13}\text{C}$ -macroalgal, is described as a linear function of the
265 independent variables X_i , as follows: $\delta^{13}\text{C}\text{-macroalgal} = a + b_1(X_1) + b_2(X_2) + \dots + b_n(X_n)$ (1). Where
266 a is regression constant (it is the value of intercept and its value is zero); b_1 , b_2 , and b_n , are regression
267 coefficients for each independent variable X_i . From each one of the fitted regression models, we
268 extracted the estimated regression coefficients for each of the predictor variables (e.g., Bayesian
269 Information Criterion (BIC), Akaike Information Criterion (AIC), root-mean-square error (RMSE),
270 Mallow's C_p criterion, F Ratio test, the p-value for the test (Prob > F), coefficients of determination

271 (R²) and the adjusted R² statistics) (Stroup et al., 2018). All regression coefficients were used as
272 indicators of the quality of the regression (Burnham and Anderson, 2002; Draper and Smith, 1998).
273 Kolmogorov-Smirnov normality test was applied for all variables, and all were normally distributed.
274 Most of the $\delta^{13}\text{C}$ values in each group showed a normal distribution. For all statistical tests, a
275 probability $P < 0.05$ was used to determine statistical significance. The statistical analysis of the
276 results was using JMP 14.0 software (SAS Institute Inc.).

277

278 **3. Results**

279 **3.1. Taxonomy and morpho-functional groups**

280 Sampled specimens belong to three Phyla, 63 genera, and 170 species. The Phyla were identified as
281 Chlorophyta (25%), Ochrophyta (22%), and Rhodophyta (53%). The most representative genus (and
282 their species) were *Ulva* (*U. lactuca*, *U. lobata*, *U. flexuosa*, and *U. intestinalis*), *Codium* (*C.*
283 *amplivesiculatum* and *C. simulans*), *Chaetomorpha* (*C. antennina*), *Padina* (*P. durvillei*), *Dictyota*
284 (*D. dichotoma*), *Colpomenia* (*C. tuberculata* and *C. sinuosa*), *Sargassum* (*S. sinicola* and *S.*
285 *horridum*), *Amphiroa* (*Amphiroa* spp.), *Spyridia* spp, *Polysiphonia* spp., *Gymnogongrus* spp.,
286 *Gracilaria* (*G. vermiculophylla*, *G. pacifica* and *G. crispata*), *Hypnea* (*H. pannosa* and *H. johnstonii*)
287 *Grateloupia* (*G. filicina* and *G. versicolor*), and *Laurencia* (*L. papillosa* and *L. pacifica*). The
288 endemic species included Chlorophyta *Codium amplivesiculatum*, Rhodophyta *Laurencia papillosa*,
289 *Chondracanthus squarrolosa*, *Gracilaria spinigera*, and *G. subsecundata*, and Ochrophyta *Cutleria*
290 *hancockii*, *Sargassum herphorizum*, *S. johnstonii*.

291 An analysis of the biogeographical diversity among sectors evidenced that P3 (43 genera of 63, 68%)
292 and C3 (63%) at north recorded the highest number of the genus, followed by C1 (38%) and P1

293 (29%) at the south, and P2 (27%) and C2 (22%). The same pattern was observed in the species
294 diversity, zones P3 (94 of 167 species, 56%) and C3 (52%) at the north, C1 (34%) and P1 (25%) at
295 the south, and C2 and P2 (19-20%) at the center.

296 The morphofunctional groups identified were 21. The most common were C-tubular (6 spp., n=69;
297 C-Blade-like (6 spp, n=55); C-Filamentous uniseriate (17 spp, n=49); C-Erect thallus (5 spp, n=33);
298 O-Compressed with branched or divided thallus (19 spp., n=92); O-Thick leathery macrophytes (12
299 spp., n=104); O-Hollow with spherical or subspherical shape (4 spp, n=87); R-Large-sized corticated
300 (57 spp., n=225); R-Filamentous uniseriate and pluriseriate with erect thallus (9 spp., n=48); and R-
301 Large-sized articulated corallines (6 spp, n=17). The diversity, in terms of presence/absence of the
302 morphofunctional groups, varied among coastline sectors, higher in C3 (16 of 21, 76%) and P3
303 (71%) at the north, followed by C1 (57%) and P1 (48%) at the south, and C2 and P2 and (42-48%)
304 at the center of both GC coastlines.

305 **3.2. $\delta^{13}\text{C}$ -macroalgal variability in function of taxonomy and morpho-functional groups**

306 The variability of $\delta^{13}\text{C}$ values in macroalgae was analyzed by taxon (phylum, genus, species) and
307 morphofunctional groups classified by habitat, coastal sector, and collection season. A complete list
308 of the results of $\delta^{13}\text{C}$ in 170 macroalgae species is provided in Supporting Information (Table SI-1).
309 Firstly, $\delta^{13}\text{C}$ values analyzed by phylum showed a unimodal distribution with a peak at $-14\pm 1.4\text{‰}$
310 (Fig 2). Ochrophyta (-21.5 to -2.2‰ , $-12.5\pm 3.7\text{‰}$), displayed significantly higher values than
311 Chlorophyta (-25.9 to -5.5‰ , $-14.5\pm 3.0\text{‰}$) and Rhodophyta (-34.6 to -4.5‰ , $-14.8\pm 3.9\text{‰}$). The
312 $\delta^{13}\text{C}$ -macroalgal values (average \pm SD) for the genus of Chlorophyta, Ochrophyta, and Rhodophyta
313 (Fig. 3) varied from $-33.8\pm 1.1\text{‰}$ for *Schizymenia* to $-7.8\pm 0.7\text{‰}$ for *Amphiroa*. Based on the highest
314 values, specimens of three Phyla showed $\delta^{13}\text{C}$ values $> -10\text{‰}$, evidenced the presence of CCM's by

315 active uptake of HCO_3^- (strategy 1) (Fig. 3). For example, *Caulerpa*, *Cladophora*, *Codium*, *Ulva* for
316 Chlorophyta *Colpomenia*, *Dictyota*, *Padina*, *Sargassum* for Ochrophyta, and *Hypnea* and
317 *Polysiphonia* for Rhodophyta showed $\delta^{13}\text{C}$ values $> -10\text{‰}$. Likewise, high $\delta^{13}\text{C}$ values were observed
318 in the calcifying macroalgae genus *Amphiroa* and *Jania*, under strategy 1 (Fig. 3c). $\delta^{13}\text{C}$ values
319 lower than -30‰ that denote uptake of CO_2 by diffusion (strategy 3), were observed only in
320 Rhodophyta *Schizymenia*, *Halymenia*, and *Gigartina*. However, most species showed large $\delta^{13}\text{C}$
321 variabilities that evidence a mechanism that uses a mix of HCO_3^- and CO_2 for photosynthesis
322 (strategy 2).

323 Multiple comparison analyses revealed significant differences in the $\delta^{13}\text{C}$ -macroalgal values among
324 genera, ordered as *Schizymenia* $<$ *Polysiphonia* $<$ *Ulva*, *Gracilaria* and *Spyridia* ($-16.1 \pm 0.6\text{‰}$ to -
325 $15.1 \pm 0.2\text{‰}$) $<$ *Gymnogongrus*, *Laurencia*, *Hypnea*, *Cladophora*, *Dictyota*, *Sargasumm*,
326 *Chaetomorpha*, and *Grateloupia* (from $-15.4 \pm 0.7\text{‰}$ to $-13.8 \pm 0.8\text{‰}$) $<$ *Codium* and *Padina* (-
327 $12.5 \pm 2.4\text{‰}$ to $-12.4 \pm 2.5\text{‰}$) $<$ *Colpomenia* and *Amphiroa* (-9.2 ± 0.3 to $-7.8 \pm 0.7\text{‰}$) ($F=16.81$,
328 $p < 0.001$).

329 Aggrupation of $\delta^{13}\text{C}$ values based on morpho-functional features is displayed in Fig. 4. The most
330 representative groups in the phylum Chlorophyta varied from $-15.8 \pm 0.3\text{‰}$ for C-Tubular to -
331 $12.4 \pm 0.5\text{‰}$ for C-Thallus erect. The phylum Ochrophyta includes O-Thick leathery with the lowest
332 mean ($-14.8 \pm 0.3\text{‰}$) and O-Hollow with a spherical or subspherical shape with the highest values (-
333 $9.2 \pm 0.3\text{‰}$). The lowest and highest $\delta^{13}\text{C}$ values for Rhodophyta were observed for R-flattened
334 macrophytes ($-24.0 \pm 9.6\text{‰}$) and R-Larger-sized articulated coralline ($-7.9 \pm 0.8\text{‰}$), respectively.
335 Significant differences were observed among groups, which were ordered as follows: R-Flattened
336 macrophytes $<$ R-Blade like $<$ C-Tubular $<$ O-Tick leathery and R-Large size corticated $<$ C-Blade
337 like and C-Filamentous uniseriate $<$ C- Thallus erect and O-Compressed with branch $<$ O-Hollow

338 with spherical < R-Larger-sized articulated coralline.

339 High intraspecific variability in $\delta^{13}\text{C}$ signal for the more representative genera of each taxon is
340 showed in Table 1-3. For *Codium*, *C. brandegeei* ($11.8\pm 1.2\%$) and *C. simulans* ($-11.4\pm 2.2\%$)
341 showed higher $\delta^{13}\text{C}$ values than *C. amplivesculatum* ($-14.4\pm 2.7\%$). *Colpomenia* species had higher
342 $\delta^{13}\text{C}$ values than the other genera, with higher values for *C. tuberculata* ($-8.7\pm 3.2\%$) than
343 *Colpomenia* sp. ($-10.9\pm 3.6\%$) and *C. sinuosa* ($-10.2\pm 2.9\%$). *Gracilaria* showed comparable $\delta^{13}\text{C}$
344 values in the four species (from $-16.4\pm 1.6\%$ for *G. pacifica* to $-15.5\pm 2.4\%$ for *Gracilaria* sp.).
345 *Hypnea* showed non-significant $\delta^{13}\text{C}$ differences in three representative species ($-16.4\pm 1.7\%$ for *H.*
346 *spinella* to $-14.9\pm 2.3\%$ for *Hypnea* sp.). *Laurencia* sp. ($-12.9\pm 1.2\%$) was higher than *L. pacifica* ($-$
347 $14.9\pm 2.2\%$), while *Padina* sp. ($-11.1\pm 1.5\%$) higher than *P. durvillei* ($-13.2\pm 2.6\%$). *Sargassum* was
348 one of the most diverse genera studied with six representative species, with $\delta^{13}\text{C}$ values ordered as
349 follow: *S. horridum* = *S. sinicola* = *S. johnstonii* (-15.5 ± 2.9 to $-15.1\pm 2.4\%$) < *S. lapazeanum* ($-$
350 $14.5\pm 1.6\%$) = *Sargassum* sp. ($-14.2\pm 2.3\%$) < *S. herphorizum* ($-13.6\pm 1.6\%$). *Spyridia* sp. ($-$
351 $17.0\pm 1.2\%$) and *S. filamentosa* ($-15.8\pm 3.8\%$) showed non-significant differences. The six
352 representative species of *Ulva* were divided into two morphological groups, filamentous and
353 laminates. Filamentous species that averaged $-16.3\pm 2.0\%$ for *U. clathrata*, $-16.0\pm 3.6\%$ for *U.*
354 *flexuosa*, $-15.7\pm 1.7\%$ for *U. acanthophora* and $-15.3\pm 2.5\%$ for *U. intestinalis* and *Ulva* laminates
355 that included *U. linza* ($-15.5\pm 2.4\%$) and *U. lactuca* ($-14.1\pm 3.1\%$). Non-significant differences were
356 observed between morphological groups and among species. A high intra-specific variability, 11-
357 28%, explains average overlapping.

358 **3.3. $\delta^{13}\text{C}$ -macroalgal variability in coastal sectors**

359 A diversity of macroalgal assemblages were documented along the GC coastlines, with differences
360 in the taxonomic composition according to their fico-floristic region. Multiple comparison analyses
361 of $\delta^{13}\text{C}$ signals evidenced significant differences between the most common genus and species of
362 macroalgae between and within assemblages grouped by coastal sector, season and collecting year
363 (Supplementary Information Tables SI-2-3). For example, genus *Padina* (e.g., *P. durvillei*) and *Ulva*
364 (e.g., *U. lactuca*), collected in C1 sector during the rainy season, showed lower $\delta^{13}\text{C}$ values than in
365 other sectors. Differences in the $\delta^{13}\text{C}$ signal are mainly related to the carbon uptake strategies of the
366 macroalgae (Fig. 5). Even though most species inhabiting the GC coastal sectors dominated
367 strategies based on active CCM's, the tendencies differed between taxa and coastal regions. Strategy
368 2 with mixing DIC sources is dominant in all regions and taxa (60-90%). Exceptions were observed
369 in the P1 (68%) and C1 (37%) regions for Ochrophyta, where the specialized strategy 1 (the HCO_3^-
370 user) was significant. Strategy 3 based on the use of CO_2 was observed in the peninsular coast in P2
371 and P3 for Rhodophyta with 2-3.3%. Overall, more negative $\delta^{13}\text{C}$ values were observed at
372 continental (C2) compared to the peninsular coastline (P1-P3) and southward than northward.

373 **3.4. $\delta^{13}\text{C}$ -macroalgal variability in function of taxonomy and habitat features and** 374 **environmental conditions**

375 Variability of $\delta^{13}\text{C}$ values for the most representative genera was evaluated by multiple comparative
376 analyses in the habitat features' function, including the substrate, hydrodynamic, and emersion level.
377 Large $\delta^{13}\text{C}$ variability observed between specimens of the same genus collected in the different
378 habits do not show any significant pattern, and non-significant differences were observed. An
379 exception was observed with the emersion level (shown in Fig. 6), where intertidal specimens
380 recorded lesser negative values than subtidal in most macroalgae genus. For example, for
381 *Hydroclathrus* (intertidal $-5.7 \pm 0.9\text{‰}$; subtidal $-11.4 \pm 5.9\text{‰}$), *Amphiroa* (intertidal -6.9 ± 1.5 ; subtidal

382 $-9.9 \pm 6.1\text{‰}$), *Hypnea* (intertidal $-13.5 \pm 2.5\text{‰}$; subtidal $-18.6 \pm 1.8\text{‰}$), and *Laurencia* (intertidal -
383 $13.5 \pm 1.3\text{‰}$; subtidal $-17.1 \pm 1.8\text{‰}$). Exceptions were observed for *Polysiphonia* (intertidal -
384 $19.7 \pm 2.2\text{‰}$, subtidal $-14.9 \pm 6.7\text{‰}$), *Spyridia* (intertidal $-16.9 \pm 3.3\text{‰}$, subtidal $-13.2 \pm 0.7\text{‰}$), and
385 *Colpomenia* (intertidal $-9.4 \pm 3.4\text{‰}$, subtidal $-7.7 \pm 1.3\text{‰}$).

386 Non-significant differences were observed for the same genera at different temperatures ranges,
387 except for *Grateloupia* (cold, $-19.2 \pm 4.7\text{‰}$, typical $-14.4 \pm 2.2\text{‰}$, warm $-14.5 \pm 2.2\text{‰}$) and
388 *Polysiphonia* (cold, $-21.0 \pm 0.4\text{‰}$, typical $-18.1 \pm 5.5\text{‰}$, warm $-17.9 \pm 2.3\text{‰}$) with more negative values
389 in colder than warmer waters ($F=6.42$, $p<0.001$). Neither significant difference was observed in $\delta^{13}\text{C}$
390 values in macroalgae specimens from the different genus in the same temperature range (Fig. 7a).

391 Significant differences were observed among the genus related to the pH level at seawater (Fig. 7b).
392 Under typical pH seawater, *Amphiroa* and *Colpomenia* were 1-2‰ more negatives than in alkaline
393 waters, while *Ulva* and *Spyridia* were 3-5‰ less negative than in acidic waters. *Amphiroa* and
394 *Colpomenia* were not collected in acidic water, and neither *Spyridia* in alkaline waters to compare.
395 Another genus also showed extremes values between alkaline (*Tacanoosca* $-7.6 \pm 1.0\text{‰}$) and acidic
396 waters (*Schizymenia* $-32.9 \pm 2.0\text{‰}$). The following order was observed in the genus collected at the
397 three pH ranges: alkaline > typical > acidic. Significant differences were observed for genus
398 *Ahnfeltiopsis*, *Caulerpa*, *Gymnogongrus*, *Padina*, and *Ulva*, with higher values at alkaline than in
399 acidic waters. Values of $\delta^{13}\text{C}$ for specimens of the same genus collected at typical pH waters are
400 mostly overlapped between alkaline and acidic seawaters. Non-significant differences in $\delta^{13}\text{C}$ values
401 were observed for *Grateloupia*, *Hypnea*, and *Polysiphonia* concerning pH-type waters.

402 We analyzed the carbon uptake strategies on macroalgal assemblages in the function of
403 environmental factors like temperature, pH, and salinity (Fig. 8). The temperature and salinity non-

404 significantly explained the $\delta^{13}\text{C}$ -macroalgal variability. A poor but significant correlation was
405 observed between $\delta^{13}\text{C}$ and pH ($R^2 = 0.04$) (Table 4). The proportion of specimens with a strategy
406 of only HCO_3^- use was different between environmental factors and taxa (previously described). For
407 example, Ochrophyta showed the highest proportion (35%) in colder temperatures, in pH-Alkaline
408 (31%), and at a typical salinity regimen (27%). Chlorophyta was enhanced to 30% in acid pH, and
409 Rhodophyta recorded 21% at normal seawater. The opposite strategy (only use of dissolved CO_2)
410 was observed only in Rhodophyta. The highest percentage was observed in the estuarine salinity
411 regimen (10%).

412 **3.5. Variation latitudinal of $\delta^{13}\text{C}$ -macroalgal**

413 The $\delta^{13}\text{C}$ -macroalgal variation in the GC biogeography was evaluated by linear regression analysis
414 between $\delta^{13}\text{C}$ values along the nine degrees latitude in both GC coastlines. A non-significant
415 latitudinal trend was observed for datasets, but for the three phyla's most representative genera, $\delta^{13}\text{C}$
416 values correlated with latitude (Fig. 9). In Chlorophyta, with the higher genera number, $\delta^{13}\text{C}$ values
417 increased with latitude, with low but significant correlation. Contrarily, in Ochrophyta and
418 Rhodophyta specimens, the $\delta^{13}\text{C}$ values decreased non-significantly with latitude.

419 In the most representative morphofunctional groups, significant correlations ($p < 0.001$) were
420 observed for $\delta^{13}\text{C}$ -macroalgal *versus* latitude (Fig. 10). Representative morphofunctional groups of
421 Chlorophyta (e.g., C-Tubular, C-Filamentous uniseriate), showed a positive correlation, while those
422 belonging to Ochrophyta (e.g., O-Thick leathery;) and Rhodophyta (e.g., R-Large sized corticated)
423 showed a negative trend with latitude.

424 **3.6. Analyses of $\delta^{13}\text{C}$ macroalgal variability**

425 The $\delta^{13}\text{C}$ -macroalgal variability was analyzed in function of the life form and environmental factors.

426 Firstly, simple linear regression analyses were performed to evaluate the dependent variable's
427 prediction power ($\delta^{13}\text{C}$ -macroalgal) in the function of several independent variables controlling the
428 main macroalgae photosynthesis drivers (light, DIC, and inorganic nutrients). Regression
429 coefficients were estimated for each fitted regression model, which is used as indicators of the quality
430 of the regression (Burnham and Anderson, 2002; Draper and Smith, 1998) as was described in
431 Methods; however, our results description focused on the coefficients of determination (R^2 and
432 adjusted R^2). The coefficient R^2 describes the relationship between the independent variables X_i with
433 the dependent variable Y ($\delta^{13}\text{C}$ -macroalgal). R^2 is interpreted as the % of contribution to the $\delta^{13}\text{C}$
434 variability. In comparison, the adjusted R^2 statistics compensate for possible confounding effects
435 between variables.

436 Results of the analysis of the relationships between $\delta^{13}\text{C}$ with each independent variable are
437 summarized in Table 4. Phyla explain only 8% variability regarding the inherent macroalgae
438 properties, the morphofunctional properties 35%, genus 46%, and species 57%.

439 The biogeographical collection zone, featured by coastline (continental vs. peninsular) and coastal
440 sectors (C1-C3 and P1-P3), explained a maximum of 5% variability. Only the emersion level (6%)
441 contributed to the $\delta^{13}\text{C}$ variability related to the habitat features. The contribution of the seawater's
442 environmental conditions was marginal for pH (4%) and negligible for temperature and salinity. A
443 marginal reduction in the percentage of contribution was observed for Phyla (1%) and
444 morphofunctional properties (1%), but significant for genus (5%) and species (10%).

445 Multiple regression analyses were also performed to interpret the complex relationships among $\delta^{13}\text{C}$ -
446 macroalgal, considering the life form (morphofunctional and taxon by genus) and their responses to
447 environmental parameters. Results for the fitted regression models performed for morphofunctional
448 groups (Table 5) and genus (Table 6) evidenced that the effect of the coastal sector and pH ranges

449 on the $\delta^{13}\text{C}$ -macroalgal increased the contribution by 9-10% each one. The emersion level increased
450 by 5-6%, the contribution respect to individual effect of morphofunctional group and genus, the
451 temperature and pH in 1 and 3%, respectively, while salinity decreased by 1-2%. The combined
452 effect of the biogeographical collection zone (e.g., coastline sector) and morphofunctional group
453 (Table 5) and genus (Table 7), increased in 11-12%.

454 Considering the combined effect of the coastline sector + Habitats features for Morphofunctional
455 group or Genus (Table 7), the full model showed R^2 of 0.60 and 0.71. In contrast, Coastline sector +
456 Environmental conditions + Morphofunctional group or Genus the R^2 increased to 0.62 and 0.72,
457 respectively. The interactive explanations of environmental factors increased the explanation
458 percentage of $\delta^{13}\text{C}$ variability; however, these contributions were significantly lower than the
459 explained by life forms, such as the morphofunctional properties and taxa by genus and species.

460 The combined effect of environmental conditions on the $\delta^{13}\text{C}$ variability was tested for the best-
461 represented genus and morphological groups. Results evidenced that 9 of 21 morphological groups
462 showed significant effects on the $\delta^{13}\text{C}$ variability (Table 8), five increasing and four decreasing the
463 model constant of $\delta^{13}\text{C} = -14.2\text{‰}$. For example, for the O-Hollow with spherical or subspherical shape
464 (+4.9‰) and R-Larger-sized articulated corallines (+6.3‰), the predicted values are $-7.9 \pm 0.8\text{‰}$ and
465 $-9.2 \pm 0.4\text{‰}$. For R-Filamentous uniseriate and pluriseriate with erect thallus (-2.1‰) and C-Tubular
466 (-1.6‰), the predicted values are $-16.3 \pm 0.5\text{‰}$ and $-15.8 \pm 0.5\text{‰}$, respectively. Regarding taxon, a
467 significant effect was observed only in 13 genera, including *Colpomenia* (+5.4‰), *Amphiroa*
468 (+6.8‰), and *Padina* (+2.2‰) increasing the signal, and *Polysiphonia* (-3.7‰), *Gracilaria* (-0.9‰),
469 and *Spyridia* (-1.4‰) decreasing the signal of the model constant (Table 9). In 33 species was
470 observed a significant effect on the $\delta^{13}\text{C}$ variability, including *C. tuberculata* +5.9‰, *C. sinuosa*
471 +4.4‰, *H. pannosa* +4.4‰, *H. johnstonii* +4.4‰, and *Amphiroa* spp. (+4.4 to 8.2‰) increasing the
472 model constant $\delta^{13}\text{C} = -14.6\text{‰}$, and *Spyridia* sp. (-2.5‰), *G. filicina* (-2.3‰), *P. mollis* (-5.2‰) and

473 *S. pacifica* (-19.2‰) (Table 10).

474

475 **3.7. Preliminary estimations of $\Delta^{13}\text{C}$ -macroalgal**

476 Concurrent analysis of surface seawater for alkalinity, proportions of the chemical species of DIC
477 (CO_2 , HCO_3^- , and CO_3^{2-}), and $\delta^{13}\text{C}$ -DIC evidenced that $\delta^{13}\text{C}$ -DIC in GC seawater averages
478 $1.4 \pm 0.4\text{‰}$ (-1 to 4.9‰) (Supplementary Information Fig. SI-1). In our preliminary data, the $\delta^{13}\text{C}$ -
479 DICseawater slightly (in 0.5‰) decreased during the rainy season in those zones influenced by river
480 discharges along the continental coastline. Non-significant differences were observed among coastal
481 sectors. $\delta^{13}\text{C}$ -DIC values in GC seawater are comparable to the averages 1.4 - 1.6‰ reported for the
482 surface seawaters in the Eastern North Pacific in the 1970s-2000s (Hinger et al., 2010; Quay et al.,
483 2003; Santos et al., 2011).

484 Based on the subtraction of $\delta^{13}\text{C}$ macroalgae to $\delta^{13}\text{C}$ -DICseawater, the integrative discrimination
485 factor against ^{13}C averaged $16.0 \pm 3.1\text{‰}$, $16.8 \pm 4.3\text{‰}$, and $14.0 \pm 3.8\text{‰}$ for Phyla Chlorophyta,
486 Rhodophyta, and Ochrophyta, respectively. Five groups were identified in the function of the $\Delta^{13}\text{C}$
487 values, one for Chlorophyta ($\Delta^{13}\text{C} = 16.0 \pm 3.1\text{‰}$), two for Rhodophyta ($16.6 \pm 3.8\text{‰}$ and $34.6 \pm 1\text{‰}$),
488 and two for Ochrophyta ($9.1 \pm 1.7\text{‰}$ and $15.7 \pm 2.7\text{‰}$) (Fig. S2). Values of $\Delta^{13}\text{C}$ were comparable to
489 $\delta^{13}\text{C}$ of the thallus of macroalgae. Thus, $\delta^{13}\text{C}$ -macroalgal reflect mainly the discrimination during
490 carbon assimilation. Like $\delta^{13}\text{C}$ -macroalgal, the $\Delta^{13}\text{C}$ values were subject to considerable variation.

491

492 **4. Discussions**

493 **4.1. Explaining the $\delta^{13}\text{C}$ macroalgal variability**

494 A high variability in the $\delta^{13}\text{C}$ values was revealed in the large inventory of macroalgae collected
495 along the GC coastline. A linear regression analysis of the effects of life forms revealed that the $\delta^{13}\text{C}$
496 variability in the macroalgal community is mainly explained by taxonomic (genus 46%, species
497 57%) and morphofunctional groups (35%). This result is consistent with Lovelock et al. (2020)
498 report, which found that 66% of $\delta^{13}\text{C}$ variability was explained by taxonomy. Even so, the variability
499 associated with each genus is not the same and can be classified in three groups: 1) high variability
500 (e.g., *Schizymenia* $=\pm 19.1\text{‰}$), moderate variability (e.g., *Hydroclathrus* $=\pm 7.3\text{‰}$; *Amphiroa*
501 $=\pm 6.8\text{‰}$) and low variability (e.g., *Gracilaria* $=\pm 0.89$; *Spyridia* $=\pm 1.46\text{‰}$). The observed $\delta^{13}\text{C}$
502 variability in this study is comparable with those reported in the literature, compiled in Table SI-4.

503 Most authors studying the isotopic composition of C in macroalgae have reported the high isotopic
504 variability, which has been attributable to the taxon-specific photosynthetic DIC acquisition
505 properties (Díaz-Pulido et al., 2016; Lovelock et al., 2020; Marconi et al., 2011; Mercado et al.,
506 2009, Raven et al., 2002a; Stepien, 2015)). Our study observed that the intrinsic characteristics of
507 each morpho-functional group of macroalgae (e.g., thallus structure, growth form, branching pattern,
508 and taxonomic affinities) also influence the $\delta^{13}\text{C}$ -macroalgal signals. The thallus thickness,
509 morphology propriety influences the diffusion boundary layer on the surface of the macroalgal,
510 where they carry out the absorption of essential ions and dissolved gases (Hurd, 2000; SanFord and
511 Crawford, 2000). Thus, morphology can modulate the photosynthesis rates. However, a non-
512 biological or ecological explanation of the $\delta^{13}\text{C}$ variability, and therefore carbon use physiology, can
513 be given in terms of morphology.

514 The $\delta^{13}\text{C}$ -macroalgal depends on the carbon source ($\delta^{13}\text{C}$ -DIC in seawater), the isotope
515 discrimination during carbon assimilation in the photosynthesis ($\Delta^{13}\text{C}_p < 29\text{‰}$ in a variable degree),
516 and the plant respiration ($\Delta^{13}\text{C}_r$ average $\pm 2.3\text{‰}$) (Carvalho et al., 2009a,b; 2010a; Carvalho and Eyre,

517 2011; Rautenberger et al., 2015). Comparatively, the $\Delta^{13}\text{C}_r$ value is relatively small regarding $\Delta^{13}\text{C}_p$.
518 Thus, $\delta^{13}\text{C}$ -macroalgal is an integrative value of the isotope discrimination during DIC seawater
519 assimilation [$\Delta^{13}\text{C} = (\delta^{13}\text{C}\text{-DIC seawater} - \delta^{13}\text{C}_{\text{macroalgae}})$] (Carvalho et al., 2009a). Based on the
520 $\Delta^{13}\text{C}$ values, five groups were identified in our study: one for Chlorophyta ($\Delta^{13}\text{C} = 16.0 \pm 3.1\%$), two
521 for Rhodophyta ($16.6 \pm 3.8\%$ and $34.6 \pm 1\%$), and two for Ochrophyta ($9.1 \pm 1.7\%$ and $15.7 \pm 2.7\%$).
522 Values of $\Delta^{13}\text{C}$ were comparable to $\delta^{13}\text{C}$ of the thallus of macroalgae. The $\delta^{13}\text{C}$ -macroalgal values
523 reflect the discrimination during carbon assimilation attributable to the taxon-specific photosynthetic
524 DIC acquisition properties. $\Delta^{13}\text{C}$ -macroalgal variability, captured in the $\delta^{13}\text{C}$ -macroalgal signals, is
525 related to the thickness of the boundary layer around the thallus (Raven et al., 1982), the leakage
526 during carbon uptake (Maberly et al., 1992; Sharkey and Berry 1985), photosynthetic intensity
527 (Kübler and Raven 1995, 1996; Wiencke and Fischer 1990), and respiration rates (Carvalho et al.,
528 2010a; Carvalho and Eyre, 2011; Rautenberger et al., 2015). All intrinsic properties are related to
529 the life form.

530 Many species that recorded high $\delta^{13}\text{C}$ values (and low $\Delta^{13}\text{C}$ values) were fleshy macroalgae that are
531 characterized to be bloom-forming macroalgae belonging to genera *Ulva*, *Gracilaria*, *Cladophora*,
532 *Spyridia*, and *Sargassum* (Páez-Osuna et al., 2013; Valiela et al., 2018). It is not surprising that
533 species with high photosynthetic activity and high relative growth rates (Hiraoka et al., 2020) have
534 high carbon demand that results in lower isotopic discrimination against ^{13}C (Carvalho et al., 2010ab;
535 Cornelisen, et al., 2007; Kübler and Dungeon, 2015; Rautenberger et al., 2015). Bloom-forming
536 macroalgae (e.g., *Ulva*, *Gracilaria*, *Sargassum*) have been remarked as facultative species capable
537 of switching from C3 to C4 pathway (Valiela et al., 2018). C4 pathway reduces photorespiration, the
538 antagonist process of RuBisCo, enhancing the DIC assimilation in 25-40% and increasing the $\delta^{13}\text{C}$
539 values (Bauwe et al., 2010; Ehleringer et al., 1991; Zabaleta et al., 2012). C4 pathway has more

540 energy investment in CCM's than in RuBisCo protein content than C3 pathway (Young et al., 2016).
541 Also, the reports of C4 or C4-like pathway features in algae have increased in the last years
542 (Doubnerová and Ryslavá, 2011; Roberts et al., 2007; Xu et al., 2012, 2013). For example, high
543 activity of key enzymes of C4 metabolisms, such as pyruvate orthophosphate dikinase (PPDK),
544 phosphoenolpyruvate carboxylase (PEPC), and phosphoenolpyruvate carboxykinase (PCK), has
545 been described in many algae species. But the establishment of a true C4 pathway in marine algae is
546 not clear since the massive changes in gene expression patterns seem to be incomplete, and it is
547 suggested that many marine algae have high plasticity to use a combination of CCM to overcome Ci
548 limitations (Doubnerová and Ryslavá, 2011; Roberts et al., 2007; Xu et al., 2012, 2013). A Stepwise
549 model of the path from C3 to C4 photosynthesis is explained by Gowik and Westhoff (2011). More
550 research is required on this topic considering the increasing the frequency, intensity, and extension
551 of bloom-forming macroalgae events worldwide (Teichberg et al., 2010; Valiela et al., 2018) and in
552 México (Ochoa-Izaguirre et al., 2007; Ochoa-Izaguirre and Soto-Jiménez, 2015; Páez-Osuna et al.,
553 2017).

554 Changes in the habitat features and environmental conditions, such as light intensity and DIC
555 availability, influencing the growth rate and photosynthetic intensity, have a strong influence on $\delta^{13}\text{C}$
556 signal (Carvalho et al., 2007, 2009a; Carvalho and Eyre, 2011; Mackey et al., 2015; Rautenberger et
557 al., 2015; Stepien, 2015). The light intensity is the external factor with more influence on the $\Delta^{13}\text{C}$ -
558 macroalgal due to the regulation of carbon assimilation intensity (Carvalho et al., 2009a,b; Cooper
559 and DeNiro 1989; Grice et al., 1996). Experimental studies found the light levels as a critical factor
560 affecting the $\delta^{13}\text{C}$ values. For example, under saturating light conditions, *Ulva* switched from a
561 carbon uptake of HCO_3^- and CO_2 to increased HCO_3^- use (Rautenberger et al., 2015). Furthermore,
562 field studies have shown that species growing in low light habitats as deep subtidal tend to have

563 more negative $\delta^{13}\text{C}$ values than those in higher light environments (Cornwall et al., 2015; Díaz-
564 Pulido et al., 2016; Hepburn et al., 2011; Marconi et al., 2011; Mercado et al., 2009; Stepien 2015).
565 In this study, intertidal specimens recorded lesser negative values than subtidal in most macroalgae
566 genus. However, our study did not record the vertical effect in the $\delta^{13}\text{C}$ signal related to the light
567 limitation because only shallow habitats (non-light limited) were studied.

568 $\delta^{13}\text{C}$ -DICseawater is reasonably uniform in surface seawater (-4.8 to 3.6‰, median 1.5‰), with
569 $\delta^{13}\text{C}$ values for CO_2 , HCO_3^- , and CO_3^{2-} nearly -10, -0.5 and 2‰, respectively (Kroopnick, 1985;
570 Mook et al., 1974). Exceptions can be expected where variations in the salinity, alkalinity, and
571 proportions of the chemical species of DIC (CO_2 , HCO_3^- or CO_3^{2-}) occur (e.g., in coastal
572 environments influenced by river and groundwater discharges) (Carvalho et al., 2015; Chanton and
573 Lewis 1999; Hinger et al., 2010; Mook et al., 1974). Regarding DIC sources for macroalgae in the
574 GC surface seawater, the availability, chemical proportions, and $\delta^{13}\text{C}$ -DIC were also relatively
575 constant and uniform. Thus, the influence of the $\delta^{13}\text{C}$ -DIC variations on the $\delta^{13}\text{C}$ -macroalgal
576 variability is negligible in the GC.

577 The effect of other environmental factors, such as salinity and pH, on $\delta^{13}\text{C}$ -macroalgal signals, was
578 evaluated. Regarding salinity, the influence of freshwater discharge by rivers and groundwater
579 decreases the $\delta^{13}\text{C}$ signal, which could be explained by the reduction in the salinity regimen that
580 follows a decrease in $\delta^{13}\text{C}$ -DIC in water (Hinger et al., 2010; Santos et al., 2011). In our study, a
581 non-significant correlation between $\delta^{13}\text{C}$ -macroalgal and salinity was observed.

582 Based on pH, differences in $\delta^{13}\text{C}$ were found only for a few genera (e.g., *Amphiroa*, *Colpomenia*,
583 *Ulva*, *Spyridia*), with a trend to increase in the $\delta^{13}\text{C}$ values with pH increase, such as was reported
584 by Maberly et al. (1992) and Raven et al. (2002b). Similar results were reported for Cornwall et al.

585 (2017) in the field study, with the differential response of the $\delta^{13}\text{C}$ signals to pH among 19 species,
586 in which only four species were sensitive to pH changes. A very weak but significant positive linear
587 regression was observed between $\delta^{13}\text{C}$ and pH. Also, a trend to decrease in the $\delta^{13}\text{C}$ was recorded in
588 the following order: alkaline > typical > acidic. According to Stepien (2015), the result of meta-
589 analyses between pH drift experiments and $\delta^{13}\text{C}$ thresholds was positive only for Rhodophyta and
590 Ochrophyte but not for Chlorophyta. About 86% of the Stepien metadata met the theoretical CCM
591 assignment based on both parameters, exceptions for species with $\delta^{13}\text{C} < -30\text{‰}$ that have been capable
592 of raising pH > 9. A strong association between pH compensation point and $\delta^{13}\text{C}$ was reported by
593 Iñiguez et al. (2019) in three taxa of polar macroalgae. Environmental conditions may influence the
594 $\delta^{13}\text{C}$ -macroalgal values but not change the carbon use physiology in the macroalgae, which is most
595 likely inherently species-specific.

596 **4.2. Using $\delta^{13}\text{C}$ -macroalgal to indicate the presence of an active CCM**

597 In our study, the $\delta^{13}\text{C}$ macroalgae signals were used to evidence the presence of an active CCM. This
598 tool was first used in macroalgal shallows communities of the GC. Most macroalgae species
599 displayed $\delta^{13}\text{C}$ values that exhibit active CCM's. Then, macroalgae were classified into three
600 strategies for DIC uptake, in agreement with the Maberly et al. (1992) and Raven et al. (2002a)
601 thresholds: 1) CCM-only by active uptake HCO_3^- ($\delta^{13}\text{C} > -10\text{‰}$), 2) CCM active uptake HCO_3^- and
602 diffusive uptake CO_2 ($\delta^{13}\text{C} < -11$ to -30‰), and 3) Non-CCM, CO_2 by diffusion only ($\delta^{13}\text{C} < -30\text{‰}$).
603 About 84% of the analyzed specimens showed the facultative uptake of HCO_3^- and CO_2 , the most
604 common strategy identified in macroalgal shallow communities (Cornwall et al., 2015; Díaz-Pulido
605 et al., 2016; Hepburn et al., 2011; Stepien 2015). Based on the carbon uptake strategies, the most
606 abundant macroalgae were those able to use both HCO_3^- and CO_2 using active uptake plus passive
607 diffusion (strategy 2).

608 Macroalgae collected in GC also involved only HCO_3^- users (strategy 1) and those relying on
609 diffusive CO_2 uptake (strategy 3). Photosynthesis that relies on CO_2 uptake (lack of CMM), the most
610 primitive mechanism (Cerling et al., 1993), has fewer energy costs than HCO_3^- uptake, which
611 requires complex machinery with a high operational cost (Giordano et al., 2005; Hopkinson et al.,
612 2011; Hopkinson et al., 2014; Raven and Beardall, 2016). The energy for macroalgae to uptake
613 HCO_3^- , cross the plasma membrane, and convert to CO_2 for photosynthesis, is obtained through
614 irradiance (Cornelisen et al., 2007). Based on our sampling effort, focused on intertidal and shallow
615 subtidal habitats featured by high-light intensities, we expected high proportions of species with the
616 carbon uptake strategy that uses only HCO_3^- . Results evidenced that strategy 1 was recorded in
617 specimens belonging to 58 species of 170 total species. The higher proportions of CCM species
618 (HCO_3^- users) with high-energetic requirements are explained by those elevated irradiances
619 (Cornwall et al., 2015; Hepburn et al., 2011). Ochrophyta showed the highest proportion of species
620 that depend only on HCO_3^- uptake on both coastlines in the southern region of GC (P1, C1). The low
621 solubility of CO_2 is related to high temperatures in subtropical waters (Zeebe and Wolf-Gladrow,
622 2001) that impulse the development of CCM (Raven et al., 2002b) and by the high affinity to DIC
623 by Ochrophyta, such as has been described before by Diaz-Pulido et al. (2016).

624 Only three non-calcifying species (*Schizymenia pacifica*, *Halymenia* sp., *Gigartina* sp.) belonging
625 to Rhodophyta were CO_2 exclusive users ($\delta^{13}\text{C}=-33.2\pm 1\%$). Based on measurements of pH drift,
626 Murru and Sandgren (2004) reported *Schizymenia pacifica* and two species of *Halymenia* (e.g., *H.*
627 *schizymenioides* and *H. gardner*) as restricted CO_2 users. Measurements of $\delta^{13}\text{C}$ in *Halymenia*
628 *dilatate* confirmed the CO_2 -restricted photosynthesis in specimens collected offshore in deep reefs
629 of the Great Barrier reef (Díaz-Pulido et al., 2016). Red macroalgae that lack CCM, tend to inhabit
630 low-light habitats like subtidal or low intertidal and are abundant in cold waters (Cornwall et al.,

631 2015; Raven et al., 2002a). According to these authors, approximately 35% of the total red algae
632 tested globally are strictly CO₂ dependents. The percentage of macroalgae species representative of
633 Arctic and Antarctic ecosystems that lack CCM is 42-60% (Iñiguez et al., 2019; Raven et al., 2002b),
634 50% for temperate waters of New Zealand (Hepburn et al., 2011), and up to 90% found for a single
635 site of Tasmania, Australia (Cornwall et al., 2015). Our study sampled 91 red macroalgae species
636 (of 453 red macroalgae species reported in the GC, Pedroche and Senties, 2003), of which <3% were
637 CO₂ dependents. This low percentage could be related to the fact that deep habitats (>2 m depth low
638 tide) were not explored in our surveys.

639 Few calcifying macroalgae species using HCO₃⁻ were also collected, including the genera *Amphiroa*
640 (-7.8±3.7‰) and *Jania* (-9.4±0.7‰), both Rhodophyta with articulated-form. *Padina*, a genus with
641 less capacity to precipitate CaCO₃ (Ilus et al., 2017), displayed relatively high δ¹³C values (-
642 12.5±2.4‰), suggesting the presence of CCM using HCO₃⁻. Some species of *Padina* can use HCO₃⁻
643 , but their efficiency may differ from species to species (Enríquez and Rodríguez-Román, 2006;
644 Raven et al., 2002a). Stepien (2015) reported a global mean of -14.8±1.0‰ for calcifying species
645 compared to -20.1±0.3‰ for non-calcifying species. Calcifying macroalgae species showed a δ¹³C
646 signal indicative of HCO₃⁻ use, the same source described as the substrate for calcification (Digby
647 1977, Roleda et al., 2012) and other sources as respiratory CO₂ for the calcifying process
648 (Borowitzka and Larkum 1976). Also, the boundary layers acidified by an excess of H⁺ released as
649 residuals products of the calcifying benefit the HCO₃⁻ uptake (Comeau et al., 2012; McConnaughey
650 et al., 1997). Another possibility to explain high δ¹³C values can also be related to the highly efficient
651 light properties enhanced by the carbonate skeleton, resulting in an optimization of photosynthetic
652 activity (Vásquez-Elizondo et al., 2017). Hofmann and Heesch (2018) reported high δ¹³C values in
653 eight rhodoliths species (calcifying species) for the organic matter thallus and for thallus, including

654 CaCO₃ structure collected in deep habitats (25-40 m) where light availability is limited. Because the
655 ocean acidification in progress, negative impacts are expected on calcifying organisms, more
656 attention as ecological sentinels is warranted in the GC.

657 Measurements of $\delta^{13}\text{C}$ signal evidence of the presence or absence of CCMs in macroalgae and
658 indicate carbon use physiology (Giordano et al., 2005). However, the isotopic signature may be
659 inconclusive in determining of the efficient use of one or more DIC species (CO₂ and HCO₃⁻) (Roleda
660 and Hurd, 2012). The preferential DIC uptake of macroalgae is assessed by pH drift experiments
661 (Fernández et al., 2014; Fernández et al., 2015; Hepburn et al., 2011; Narvarte et al., 2020; Roleda
662 and Hurd, 2012). Also, it can be determined by simultaneously measuring the CO₂ uptake and O₂
663 production rates using membrane-inlet mass spectroscopy (MIMS) (Burlacot et al., 2020; Douchi et
664 al., 2019). Macroalgae that are unable to raise the seawater pH>9.0 are primarily CO₂-users, while
665 those that can raise the seawater pH>9.0 (absence of CO₂) are HCO₃⁻-users (Roleda and Hurd, 2012).
666 Those differences in the carbon uptake strategies can be easily deduced by pH drift experiments,
667 which were not done in our study but reported in the literature (Supplementary Information Table
668 SI-4). Also, the change in $\delta^{13}\text{C}$ signature within the range specific to a carbon use strategy (e.g., mix
669 HCO₃/CO₂-user) can be complemented by simultaneous measurements of O₂ and CO₂ produced
670 and consumed, respectively using MIMS. For example, photosynthetic O₂ production in a certain
671 macroalgae species with an active CCM preferring (e.g., CO₂) is about ten times higher than no
672 active CCM (Burlacot et al., 2020).

673 Based on the $\delta^{13}\text{C}$ values, it is possible to assume that at least one basal CCM is active. However, it
674 is not possible to discern what type of CCM is expressed in the organisms (e.g., direct HCO₃⁻ uptake
675 by the anion-exchange protein AE; Drechsler and Beer, 1991; Drechsler et al., 1993) or types of
676 mitochondrial carbonic anhydrase (e.g., internal and external) that enhance the fixation of Ci by

677 recycling mitochondrial CO₂ (Bowes, 1969; Jensen et al., 2020; Zabaleta et al., 2012). Also, the co-
678 existence of different CCMs has been described for the same species (Axelsson et al., 1999, Xu et
679 al., 2012), even that different CCM's can operate simultaneously, generating different Ci
680 contributions to RuBisCo internal pool (Rautenberger et al., 2015). The variety of CCMs and their
681 combinations could contribute to the high $\delta^{13}\text{C}$ variability for the same species. In our field study, it
682 is impossible to explain the variations of $\delta^{13}\text{C}$ or $\Delta^{13}\text{C}$ -macroalgal relative to CCM or CA activity
683 types. Controlled experiments, like those conducted by Carvalho and collaborators (e.g., Carvalho
684 et al. 2009a,b, Carvalho et al., 2010a), are required to obtain this knowledge.

685 **4.3. Variability of $\delta^{13}\text{C}$ macroalgal between the GC bioregions**

686 Changes in the $\delta^{13}\text{C}$ signal with latitude, mainly related to the light and temperature, have been
687 reported in the literature (Hofmann and Heesch, 2018; Lovelock et al., 2020; Marconi et al., 2011;
688 Mercado et al., 2009; Stepien, 2015). For example, a negative correlation between latitude and $\delta^{13}\text{C}$ -
689 macroalgal was described by Stepien (2015). The authors concluded that the $\delta^{13}\text{C}$ signal increased
690 by 0.09‰ for each latitude degree from the Equator. Hofmann and Heesch (2018) showed a robust
691 latitudinal effect to decrease in $\delta^{13}\text{C}$ signals ($R^2= 0.43 \delta^{13}\text{C}_{\text{total}}$ and 0.13, for $\delta^{13}\text{C}_{\text{organic-tissue}}$, $p=0.001$)
692 for rhodolite and macroalgae from coral reefs in Australia. In both cases, the latitude range is higher
693 than we tested (30° to 80° and from 10° to 45°, respectively). These differences on a big scale tend
694 to be associated with a temperature effect (Stepien, 2015) and their effect on CO₂ solubility in
695 seawater (Zeebe and Wolf-Gladrow, 2001). However, in our study, no geographical pattern in the
696 $\delta^{13}\text{C}$ macroalgal was observed. Our linear regression analyzes for latitudes showed a low but
697 significant correlation for the dataset classified by morphofunctional groups and genus, negative in
698 the cases of Rhodophyta and Ochrophyta groups, and positive for Chlorophyta.

699 Light is not limited along the GC latitudes. Most of the shallow habitats occupied by macroalgal
700 communities in the GC were high-light environments. In agreement with the literature, the surface
701 seawater temperature across the GC varies in only 1°C annual mean (Escalante et al., 2013, Robles-
702 Tamayo, 2018). However, larger temperature variations of 5-10°C were recorded in the coastal
703 waters across the GC bioregions in both climatic seasons. The combined effect of the coastline
704 sector, habitats feature, or environmental condition for Morphofunctional group or Genus explained
705 60-62 and 71-72% of the $\delta^{13}\text{C}$ variability, respectively. Our analysis of variability for the best-
706 represented morphological groups (e.g., R-Filamentous uniseriate and pluriseriate with erect thallus
707 and C-Tubular) and genus (e.g., *Colpomenia*, *Padina*, *Polysiphonia*, and *Gracilaria*) revealed that
708 certain life forms are better monitors explaining the variability of $\delta^{13}\text{C}$ -macroalgal (and $\Delta^{13}\text{C}$ values)
709 than others. The $\delta^{13}\text{C}$ variability in morphological groups refers to change within a specific carbon
710 use strategy, but not change in the carbon use physiology that is inherently species-specific. The
711 biological or ecological relevance of the $\delta^{13}\text{C}$ variability in function of the morphology, in terms of
712 the efficiency in the use of DIC and the isotope discrimination during carbon assimilation and
713 respiration, must be investigated in species of same genus morphologically different or between
714 same morphological structures belonging to a different taxon.

715 The proportion of specimens with different carbon uptake strategies also showed regional variations.
716 For example, the facultative uptake of HCO_3^- and CO_2 was dominant in the macroalgal shallow
717 communities in the GC (60 to 90% of specimens). Exceptions were observed for Ochrophyta in the
718 P1 (68%) and C1 (37%) regions, where the strategy using only HCO_3^- dominated. While the strategy
719 based on only use of CO_2 was observed in the peninsular coast in P2 and P3 for Rhodophyta with 2-
720 3.3%. Finally, the coastal sector C2 showed more negative $\delta^{13}\text{C}$ values in macroalgae specimens of
721 the same genus compared to the peninsular coastline (P1-P3). Small but detectable changes were

722 observed in the Phyla distribution based on environmental conditions. For example, Ochrophyta
723 showed the highest proportion (35%) in colder temperature, in pH-Alkaline (31%), and at typical
724 salinity regimen (27%), while Chlorophyta enhanced to 30% in acid pH and Rhodophyta recorded
725 21% at normal seawater. The opposite strategy (only use of dissolved CO₂) was observed only in
726 Rhodophyta. The highest percentage was observed in the estuarine salinity regimen (10%). Again,
727 more research is required to obtain valuable information on the physiological and environmental
728 status of macroalgae.

729

730 **5. Conclusions**

731 In conclusion, we observed high $\delta^{13}\text{C}$ -macroalgal variability in macroalgae communities in the Gulf
732 of California, such as reported in other worldwide marine ecosystems. The life form is the principal
733 cause of $\delta^{13}\text{C}$ -macroalgal variability, which explains up to 57%. Changes in habitat characteristics
734 and environmental conditions also influence the $\delta^{13}\text{C}$ -macroalgal variability within a specific carbon
735 use strategy. Considering the combined effect of the life form, coastline sector, and environmental
736 conditions, the full model explains up to 72% (genus) of the variability. The effect of the coastal
737 sector, pH ranges, and emersion level were significant, while for salinity and temperature, negligible.

738 Most macroalgae inhabiting in GC displayed the presence of CO₂ concentrating mechanisms to
739 uptake HCO₃⁻ for photosynthesis, 84% of the total analyzed specimens were able to use both HCO₃⁻
740 and/or CO₂ employing active uptake plus passive diffusion (strategy 2: $-10 < \delta^{13}\text{C} > -30\text{‰}$). Specimens
741 belonging to 58 species of 170 total species showed carbon uptake strategy 1 that use only HCO₃⁻.
742 A higher proportion of CCM species (HCO₃⁻ users) was expected because we focused on intertidal
743 and shallow subtidal habitats featured by high-light intensities. Only three non-calcifying species

744 (*Schizymenia pacifica*, *Halymenia* sp., *Gigartina* sp.) belonging to Rhodophyta (3%) were CO₂
745 exclusive users (strategy 3: $\delta^{13}\text{C} < -30\text{‰}$). The low percentage of CO₂ dependents versus 40-90%
746 reported for temperate regions could be related to the shallow habitat sampled in our surveys (<2 m
747 depth low tide). The calcifying macroalgae genera *Amphiroa* and *Jania* using HCO₃⁻ (high $\delta^{13}\text{C}$
748 values) were present in the macroalgal communities along with the GC. Because of the ongoing
749 ocean acidification, these calcifying organisms constitute excellent ecological sentinels in the GC.

750 Finally, diverse authors have reported significant correlations between $\delta^{13}\text{C}$ signal and latitude,
751 mainly related to the light and temperature. However, in our study's latitude range (21°-31°N), the
752 linear regression analyses showed a low correlation for the $\delta^{13}\text{C}$ -macroalgal dataset classified by
753 morphofunctional groups and genus, which was negative for Rhodophyta and Ochrophyta and
754 positive for Chlorophyta. Non-clear $\delta^{13}\text{C}$ -macroalgal patterns occur along the GC latitudes.
755 However, detectable changes were observed in the $\delta^{13}\text{C}$ -macroalgal and the proportion of specimens
756 with different carbon uptake strategies among coastal sectors. For example, the facultative uptake of
757 HCO₃⁻ and CO₂ was dominant in the macroalgal shallow communities in the GC (60 to 90% of
758 specimens), but in the P1 (68%) and C1 (37%) the only use of HCO₃⁻ was the dominant strategy.

759 Our research is the first approximation to understand the $\delta^{13}\text{C}$ -macroalgal variability in one of the
760 most diverse marine ecosystems in the world, the Gulf of California. We did not pretend to resolve
761 the intricate processes controlling the variations of $\delta^{13}\text{C}$ or $\Delta^{13}\text{C}$ -macroalgal during carbon
762 assimilation and respiration and determine the isolated influence of each environmental factor.
763 Despite the large dataset and corresponding statistical analyses, our study faces limitations due to
764 research design and because no research on $\delta^{13}\text{C}$ -macroalgal analysis was developed previously in
765 the GC. The primary deficiency is the lack of pH drift experiments to discriminate $\delta^{13}\text{C}$ signal
766 variations to the carbon uptake strategies to determine preferential DIC uptake of macroalgae (CO₂

767 or HCO_3^-). The second limitation concerns the lack of controlled experiments to discern what type
768 of CCM is expressed in macroalgae (e.g., direct HCO_3^- uptake by the anion-exchange protein AE,
769 types of mitochondrial AC, or the co-existence of different CCMs). Also, more research is required
770 to assess the biological or ecological relevance of the $\delta^{13}\text{C}$ variability in function of the morphology
771 (e.g., DIC uptake efficiency and isotope discrimination during carbon assimilation and respiration).
772 Future studies assessing the ability of macroalgae to use CO_2 and/or HCO_3^- can be assessed by pH
773 drift experiments and MIMS in the cosmopolites' species and within of genus with differences in
774 the $\delta^{13}\text{C}$ values between species (e.g., *Ulva* and *Sargassum*). Finally, controlled experiments in
775 laboratory and mesocosm type combined with field studies are required to elucidate what type of
776 CCM is expressed in macroalgae. Even so, the $\delta^{13}\text{C}$ -macroalgal was a good indicator to infer the
777 presence or absence of CCM's and identify the macroalgae lineages that could be in a competitive
778 advantage based on their carbon uptake strategy and identify their geographical distribution along
779 with GC. Under the current climate change conditions and their effects as ocean acidification
780 progresses and the bloom-forming macroalgae events increase in México and worldwide, the
781 analysis of $\delta^{13}\text{C}$ -macroalgal constitutes an excellent tool to help to predict the prevalence and shift
782 of species in macroalgal communities' focused on carbon metabolism. However, to obtain the
783 maximum benefit from isotopic tools in the carbon-use strategies study, diverse and species-specific,
784 it is necessary to use them in combination with other techniques referred to herein.

785 **6. Data Availability Statement**

786 Data set are each permanently deposited Soto-Jimenez, Martin F; Velázquez-Ochoa, Roberto; Ochoa
787 Izaguirre, Maria Julia. Earth and Space Science Open Archive ESSOAr; Washington, Nov 25, 2020.
788 DOI:10.1002/essoar.10504972.1

789 [https://search.proquest.com/openview/2060de58b217ca47495469b53ae2f347/1?pq-](https://search.proquest.com/openview/2060de58b217ca47495469b53ae2f347/1?pq-origsite=gscholar&cbl=4882998)
790 [origsite=gscholar&cbl=4882998](https://search.proquest.com/openview/2060de58b217ca47495469b53ae2f347/1?pq-origsite=gscholar&cbl=4882998)

791 **7. Author contribution**

792 Velázquez-Ochoa R. participate in the collection, processing, and analysis of the samples as a part
793 of his master's degree thesis. Ochoa-Izaguirre M.J. also participated in sample collections and
794 identified macroalgae specimens. Soto-Jiménez M.F. coordinated the research, was the graduate
795 thesis director, and prepared the manuscript with contributions from all co-authors.

796 **8. Competing interests**

797 The authors declare that they have no conflict of interest.

798 **9. Acknowledgements**

799 The authors would like to thank H. Bojórquez-Leyva, Y. Montaña-Ley, and A. Cruz-López for
800 their invaluable field and laboratory work assistance. Thanks to S. Soto-Morales for the English
801 revision. UNAM-PAPIIT IN206409 and IN208613 provided financial support, and UNAM-
802 PASPA supported MF Soto-Jimenez for Sabbatical year.

803 **10. References**

804 Abbot, I. A., and Hollenberg, G.: Marine algae of California. Standford University Press, California,
805 827pp, 1976.

806 Aguilar-Rosas, L. E., and Aguilar-Rosas, R.: Ficogeografía de las algas pardas (Phaeophyta) de la
807 península de Baja California, in: Biodiversidad Marina y Costera de México (Comisión Nacional
808 Biodiversidad y CIQRO, México), edited by: Salazar-Vallejo, S. I. and González, N. E., 197-206,
809 1993.

810 Aguilar-Rosas, L. E., Pedroche, F. F., and Zertuche-González, J. A.: Algas Marinas no nativas en la
811 costa del Pacífico Mexicano. Especies acuáticas invasoras en México, Comisión Nacional para el
812 Conocimiento y Uso de la Biodiversidad, México, 211-222, 2014.

813 Álvarez-Borrego, S.: Gulf of California., in: Ecosystems of the World, 26, Estuaries and Enclosed
814 Seas, (Elsevier, Amsterdam), Edited by: Ketchum BH., 427–449, 1983.

815 Anthony, K. R., Ridd, P. V., Orpin, A. R., Larcombe, P., and Lough, J.: Temporal variation of light
816 availability in coastal benthic habitats: Effects of clouds, turbidity, and tides, *Limnol. Oceanogr.*,
817 49(6), 2201-2211, <https://doi.org/10.4319/lo.2004.49.6.2201>, 2004.

818 Axelsson, L., Larsson, C., and Ryberg, H.: Affinity, capacity and oxygen sensitivity of two different
819 mechanisms for bicarbonate utilization in *Ulva lactuca* L. (Chlorophyta), *Plant Cell Environ.*, 22,
820 969–978, <https://doi.org/10.1046/j.1365-3040.1999.00470.x>, 1999.

821 Balata, D., Piazzini, L., and Rindi, F.: Testing a new classification of morphological functional groups
822 of marine macroalgae for the detection of responses to stress, *Mar. Biol.*, 158, 2459–2469,
823 <https://doi.org/10.1007/s00227-011-1747-y>, 2011.

824 Bastidas-Salamanca, M., Gonzalez-Silvera, A., Millán-Núñez, R., Santamaria-del-Angel, E., and
825 Frouin, R.: Bio-optical characteristics of the Northern Gulf of California during June 2008, *Int. J.*
826 *Oceanogr.*, <https://doi.org/10.1155/2014/384618>, 2014.

827 Bauwe, H., Hagemann, M., and Fernie, A. R.: Photorespiration: players, partners and origin, *Trends*
828 *Plant Sci.*, 15(6), 330–336, <https://doi.org/10.1016/j.tplants.2010.03.006>, 2010.

829 Beardall, J., and Giordano, M.: Ecological implications of microalgal and cyanobacterial CO₂
830 concentrating mechanisms, and their regulation, *Funct. Plant Biol.*, 29(3), 335–347,
831 <https://doi.org/10.1071/PP01195>, 2002.

832 Bold, C. H., and Wynne, J. M.: Introduction to the Algae: Structure and reproduction. Prentice-Hall,
833 Incorporated, 706pp, 1978.

834 Borowitzka, M. A. and Larkum, A. W. D.: Calcification in green alga *Halimeda*. III. Sources of
835 inorganic carbon for photosynthesis and calcification and a model of mechanism of calcification. *J.*
836 *Exp. Bot.* 27:879–93, 1976.

- 837 Bowes, G. W.: Carbonic anhydrase in marine algae, *Plant Physiol.*, 44:726–732,
838 <https://doi.org/10.1104/pp.44.5.726>, 1969.
- 839 Bray, N. A.: Thermohaline circulation in the Gulf of California, *J. Geophys. Res. Oceans.*, 93(C5),
840 4993–5020, <https://doi.org/10.1029/JC093iC05p04993>, 1988.
- 841 Brodeur, J. R., Chen, B., Su, J., Xu, Y. Y., Hussain, N., Scaboo, K. M., Zhang, Y., Testa, J. M. and
842 Cai, W. J.: Chesapeake Bay inorganic carbon: Spatial distribution and seasonal variability, *Front.*
843 *Mar. Sci.*, <https://doi.org/10.3389/fmars.2019.000996>, 2019.
- 844 Brusca, R. C., Findley, L. T., Hastings, P. A., Hendrickx, M. E., Cosio, J. T., and van der Heiden, A.
845 M.: Macrofaunal diversity in the Gulf of California, Biodiversity, ecosystems, and conservation in
846 Northern Mexico, 179, 2005.
- 847 Burlacot, A., Burlacot, F., Li-Beisson, Y., and Peltier, G.: Membrane inlet mass spectrometry: a
848 powerful tool for algal research, *Front. Plant Sci.*, 11, 1302,
849 <https://doi.org/10.3389/fmicb.2019.01356>, 2020.
- 850 Burnham, K. P., and Anderson, D. R.: A practical information-theoretic approach, *Model selection*
851 *and multimodel inference*, 2nd ed., Springer, New York, 2002.
- 852 Carrillo, L., and Palacios-Hernández, E.: Seasonal evolution of the geostrophic circulation in the
853 northern Gulf of California, *Estuar. Coast. Shelf Sci.*, 54(2), 157–173,
854 <https://doi.org/10.1006/ecss.2001.0845>, 2002.
- 855 Carvalho, M. C. and Eyre, B. D.: Carbon stable isotope discrimination during respiration in three
856 seaweed species, *Mar. Ecol. Prog. Ser.*, 437:41–49. <https://doi.org/10.3354/meps09300>, 2011.
- 857 Carvalho, M. C., Hayashizaki, K., Ogawa, H., and Kado, R.: Preliminary evidence of growth
858 influence on carbon stable isotope composition of *Undaria pinnatifida*, *Mar. Res. Indones.*, 32, 185-
859 188, 2007.
- 860 Carvalho, M. C., Hayashizaki, K., and Ogawa, H.: Carbon stable isotope discrimination: a possible
861 growth index for the kelp *Undaria pinnatifida*, *Mar. Ecol. Prog. Ser.*, 381, 71-82,
862 <https://doi.org/10.3354/meps07948>, 2009a.

- 863 Carvalho, M. C., Hayashizaki, K. I., and Ogawa, H.: Short-term measurement of carbon stable
864 isotope discrimination in photosynthesis and respiration by aquatic macrophytes, with marine
865 macroalgal examples, *J. Phycol.*, 45(3), 761-770, 2009b.
- 866 Carvalho, M. C., Hayashizaki, K., and Ogawa, H.: Effect of pH on the carbon stable isotope
867 fractionation in photosynthesis by the kelp *Undaria pinnatifida*, *Coast. Mar. Sci.*, 34(1), 135-139,
868 2010a.
- 869 Carvalho, M. C., Hayashizaki, K., and Ogawa, H.: Temperature effect on carbon isotopic
870 discrimination by *Undaria pinnatifida* (Phaeophyta) in a closed experimental system, *J. Phycol.*,
871 46(6), 1180-1186, <https://doi.org/10.1111/j.1529-8817.2010.00895.x>, 2010b.
- 872 Carvalho, M. C., Santos, I. R., Maher, D. T., Cyronak, T., McMahon, A., Schulz, K. G., and Eyre,
873 B. D.: Drivers of carbon isotopic fractionation in a coral reef lagoon: Predominance of demand over
874 supply, *Geoch. Cosmoch. Acta*, 153, 105-115, <https://doi.org/10.1016/j.gca.2015.01.012>, 2015.
- 875 Cerling, T. E., Wang, Y., and Quade, J.: Expansion of C4 ecosystems as an indicator of global
876 ecological change in the late Miocene, *Nature*, 361 (6410), 344-345,
877 <https://doi.org/10.1038/361344a0>, 1993.
- 878 Chanton, J. P., and Lewis, F. G.: Plankton and dissolved inorganic carbon isotopic composition in a
879 river-dominated estuary: Apalachicola Bay, Florida, *Estuaries*, 22(3), 575-583,
880 <https://doi.org/10.2307/1353045>, 1999.
- 881 CNA (Comisión Nacional del Agua): Atlas del agua en México, 2012.
- 882 Comeau, S., Carpenter, R. C., and Edmunds, P. J.: Coral reef calcifiers buffer their response to ocean
883 acidification using both bicarbonate and carbonate, *Proc. Bio. Sci.*, 280(1753), 20122374,
884 <https://doi.org/10.1098/rspb.2012.2374>, 2012.
- 885 Cooper, L. W., and DeNiro, M. J.: Stable carbon isotope variability in the seagrass *Posidonia*
886 *oceanica*: Evidence for light intensity effects, *Mar. Ecol. Prog. Ser.*, Oldendorf, 50(3), 225-229,
887 1989.
- 888 Cornelisen, C. D., Wing, S. R., Clark, K. L., Hamish Bowman, M., Frew, R. D., and Hurd, C. L.:
889 Patterns in the $\delta^{13}\text{C}$ and $\delta^{15}\text{N}$ signature of *Ulva pertusa*: interaction between physical gradients and

890 nutrient source pools, *Limnol. Oceanogr*, 52(2), 820-832, 2007.

891 Cornwall, C. E., Revill, A. T., and Hurd, C. L.: High prevalence of diffusive uptake of CO₂ by
892 macroalgae in a temperate subtidal ecosystem, *Photosynth. Res.*, 124, 181–190,
893 <https://doi.org/10.1007/s11120-015-0114-0>, 2015.

894 Cornwall, C. E., Comeau, S., and McCulloch, M. T.: Coralline algae elevate pH at the site of
895 calcification under ocean acidification, *Glob. Chang. Biol.*, 23(10), 4245-4256, 2017.

896 Dawson, E. Y.: The marine algae of the Gulf of California, *Allan Hancock Pac. Exped.*, 3(10), [i-
897 v+] 189–453, 1944.

898 Dawson, E. Y.: Marine red algae of Pacific México. Part 2. *Cryptonemiales* (cont.), *Allan Hancock*
899 *Pac. Exped.*, 17(2), 241–397, 1954.

900 Dawson, E. Y.: How to know the seaweeds, Dubuque, Iowa, USA. W.M.C. Brown. Co. Publishers.
901 197 pp, 1956.

902 Dawson, E. Y.: The marine red algae of Pacific Mexico, Part 4, Gigartinales. *Allan Hancock Pacific*
903 *Exped.*, 2, 191-343, 1961.

904 Dawson, E. Y.: Marine red algae of Pacific México. Part 7. *Ceramiales*: Ceramiaceae,
905 Delesseriaceae, *Allan Hancock Pac. Exped.*, 26(1), 1–207, 1962.

906 Dawson, E. Y.: Marine red algae of Pacific México. Part 8. *Ceramiales*: Dasyaceae, Rhodomelaceae.
907 *Nova Hedwigia*, 6, 437–476, 1963.

908 Díaz-Pulido, G., Cornwall, C., Gartrell, P., Hurd, C., and Tran, D. V.: Strategies of dissolved
909 inorganic carbon use in macroalgae across a gradient of terrestrial influence: implications for the
910 Great Barrier Reef in the context of ocean acidification, *Coral Reefs*, 35(4), 1327-1341,
911 <https://doi.org/10.1007/s00338-016-1481-5>, 2016.

912 Digby, P. S. B.: Growth and calcification in coralline algae, *Clathromorphum circumscriptum* and
913 *Corallina officinalis*, and significance of pH in relation to precipitation. *J. Mar. Biol. Ass. UK*

914 57:1095–109, <https://doi.org/10.1017/S0025315400026151>, 1977.

915 Douchi, D., Liang, F., Cano, M., Xiong, W., Wang, B., Maness, P. C., Lindblad, P. and Yu, J.
916 Membrane-Inlet Mass Spectrometry enables a quantitative understanding of inorganic carbon uptake
917 flux and carbon concentrating mechanisms in metabolically engineered cyanobacteria. *Front.*
918 *Microbiol.*, 10, 1356–1356, <https://doi.org/10.3389/fmicb.2019.01356>, 2019.

919 Doubnerová, V., and Ryšlavá, H.: What can enzymes of C4 photosynthesis do for C3 plants under
920 stress?, *Plant Sci.*, 180(4), 575–583, <https://doi.org/10.1016/j.plantsci.2010.12.005>, 2011.

921 Draper, N. R., and Smith, H.: Applied regression analysis, edited by: John Wiley and Sons (Vol.
922 326), 1998.

923 Drechsler, Z., and Beer, S.: Utilization of inorganic carbon by *Ulva lactuca*. *Plant Physiol.*, 97,
924 1439–1444, <https://doi.org/10.1104/pp.97.4.1439>, 1991.

925 Drechsler, Z., Sharkia, R., Cabantchik, Z. I., and Beer, S. Bicarbonate uptake in the marine
926 macroalga *Ulva* sp. is inhibited by classical probes of anion exchange by red blood cells, *Planta*,
927 191(1), 34–40, <https://doi.org/10.1007/BF00240893>, 1993.

928 Dreckmann, K. M.: El género *Gracilaria* (Gracilariaceae, Rhodophyta) en el Pacífico centro-sur
929 mexicano, *Monografías ficológicas*, 1, 77-118, 2002.

930 Dudgeon, S. R., Davison, I. R., and Vadas, R. L.: Freezing tolerance in the intertidal red algae
931 *Chondrus crispus* and *Mastocarpus stellatus*: Relative importance of acclimation and adaptation,
932 *Mar Biol.*, 106(3), 427–436, <https://doi.org/10.1007/BF01344323>, 1990.

933 Dudley, B. D., Barr, N. G., and Shima, J. S.: Influence of light intensity and nutrient source on $\delta^{13}\text{C}$
934 and $\delta^{15}\text{N}$ signatures in *Ulva pertusa*, *Aquat. Biol.*, 9(1), 85–93, <https://doi.org/10.3354/AB00241>,
935 2010.

936 Ehleringer, J. R., Sage, R. F., Flanagan, L. B., and Pearcy, R. W.: Climate change and the evolution
937 of C4 photosynthesis, *Trends Ecol. Evol.*, 6(3), 95–99, <https://doi.org/10.1073/pnas.1718988115>,
938 1991.

939 Enríquez, S., and Rodríguez-Román, A.: Effect of water flow on the photosynthesis of three marine

- 940 macrophytes from a fringing-reef lagoon, *Mar. Ecol. Prog. Ser.*, 323, 119–132,
941 <https://doi.org/10.3354/meps323119>, 2006.
- 942 Escalante, F., Valdez-Holguín, J. E., Álvarez-Borrego, S., and Lara-Lara, J. R.: Temporal and spatial
943 variation of sea surface temperature, chlorophyll a, and primary productivity in the Gulf of
944 California, *Cienc. Mar.*, 39(2), 203-215, 2013.
- 945 Espinoza-Avalos, J.: Macroalgas marinas del Golfo de California, *Biodiversidad marina y costera*
946 *de México (CONABIO- CIQRO, México)*, edited by: Salazar-Vallejo, S.I., González, N. E., 328–
947 357, 1993.
- 948 Espinosa-Carreón, T. L., and Valdez-Holguín, E.: Variabilidad interanual de clorofila en el Golfo de
949 California, *Ecol. Apl.*, 6(1-2), 83–92, 2007.
- 950 Espinosa-Carreón, T. L., and Escobedo-Urías, D.: South region of the Gulf of California large marine
951 ecosystem upwelling, fluxes of CO₂ and nutrients, *Environ Dev.*, 22, 42–51,
952 <https://doi.org/10.1016/j.envdev.2017.03.005>, 2017.
- 953 Fernández, P. A., Hurd, C. L., and Roleda, M. Y.: Bicarbonate uptake via an anion exchange protein
954 is the main mechanism of inorganic carbon acquisition by the giant kelp *Macrocystis pyrifera* (L
955 aminariales, Phaeophyceae) under variable pH, *J. Phycol.*, 50(6), 998-1008,
956 <https://doi:10.1111/jpy.12247>., 2014.
- 957 Fernández, P. A., Roleda, M. Y., and Hurd, C. L.: Effects of ocean acidification on the photosynthetic
958 performance, carbonic anhydrase activity and growth of the giant kelp *Macrocystis pyrifera*,
959 *Photosynth. Res.*, 124(3), 293-304, 2015.
- 960 Gateau, H., Solymosi, K., Marchand, J., and Schoefs, B.: Carotenoids of microalgae used in food
961 industry and medicine, *Mini-Rev. Med. Chem.*, 17(13), 1140–1172,
962 <https://doi.org/10.2174/1389557516666160808123841>, 2017.
- 963 Gilbert, J. Y., and Allen, W. E.: The phytoplankton of the Gulf of California obtained by the “E.W.
964 Scripps” in 1939 and 1940, *J. Mar. Res.*, 5, 89–110, [https://doi.org/10.1016/0022-0981\(67\)90008-](https://doi.org/10.1016/0022-0981(67)90008-1)
965 1, 1943.
- 966 Giordano, M., Beardall, J., and Raven, J. A.: CO₂ concentrating mechanisms in algae: mechanisms,

967 environmental modulation and evolution, *Annu. Rev. Plant Biol.*, 66:99–131,
968 <https://doi.org/10.1146/annurev.arplant.56.032604.144052>, 2005.

969 Grice, A. M., Loneragan, N. R., and Dennison, W. C.: Light intensity and the interactions between
970 physiology, morphology and stable isotope ratios in five species of seagrass. *J. Exp. Mar. Biol. Ecol.*,
971 195(1), 91-110, [https://doi.org/10.1016/0022-0981\(95\)00096-8](https://doi.org/10.1016/0022-0981(95)00096-8), 1996.

972 Gowik, U., and Westhoff, P.: The path from C3 to C4 photosynthesis, *Plant Physiol.*, 155(1), 56–63,
973 <https://doi.org/10.1104/pp.110.165308>, 2012.

974 Harris, D., Horwáth, W. R., and Van Kessel, C.: Acid fumigation of soils to remove carbonates prior
975 to total organic carbon or carbon-13 isotopic analysis, *Soil Sci. Soc. Am. J.*, 65(6), 1853-1856,
976 <https://doi.org/10.2136/sssaj2001.1853>, 2001.

977 Hepburn, C. D., Pritchard, D. W., Cornwall, C. E., McLeod, R. J., Beardall, J., Raven, J. A., and
978 Hurd, C. L.: Diversity of carbon use strategies in a kelp forest community: implications for a high
979 CO₂ ocean, *Glob. Change Biol.*, 17, 2488–2497, <https://doi.org/10.1111/j.1365-2486.2011.02411.x>,
980 2011.

981 Hinger, E. N., Santos, G. M., Druffel, E. R. M., and Griffin, S.: Carbon isotope measurements of
982 surface seawater from a time-series site off Southern California, *Radiocarbon* 52(1):69–89, 2010.

983 Hiraoka, M., Kinoshita, Y., Higa, M., Tsubaki, S., Monotilla, A. P., Onda, A., and Dan, A.: Fourfold
984 daily growth rate in multicellular marine alga *Ulva meridionalis*, *Sci. Rep.*, 10(1), 1-7, 2020.

985 Hofmann, L., and Heesch, S.: Latitudinal trends in stable isotope signatures and carbon-
986 concentrating mechanisms of northeast Atlantic rhodoliths, *Biogeosciences*, 15, 6139–6149,
987 <https://doi.org/10.5194/bg-15-6139-2018>, 2018.

988 Hopkinson, B. M., Dupont, C. L., Allen, A. E., and Morel, F. M. M.: Efficiency of the CO₂-
989 concentrating mechanism of diatoms, *Proc. Natl. Acad. Sci. U.S.A.*, 108, 3830–3837,
990 <https://doi.org/10.1073/pnas.1018062108>, 2011.

991 Hopkinson, B. M., Young, J. N., Tansik, A. L., and Binder, B. J.: The minimal CO₂ concentrating
992 mechanism of *Prochlorococcus* MED4 is effective and efficient, *Plant Physiol.*, 166, 2205–2217,
993 <https://doi.org/10.1104/pp.114.247049>, 2014.

- 994 Hurd, C. L.: Water motion, marine macroalgal physiology and production, *J. Phycol.*, 36, 453–472,
995 <https://doi.org/10.1046/j.1529-8817.2000.99139.x>, 2000.
- 996 Iluz, D., Fermani, S., Ramot, M., Reggi, M., Caroselli, E., Prada, F., Dubinsky, Z., Goffredo, S. and
997 Falin, G.: Calcifying response and recovery potential of the brown alga *Padina pavonica* under ocean
998 acidification, *ACS Earth Space Chem.*, 1(6), 316–323,
999 <https://doi.org/10.1021/acsearthspacechem.7b00051>, 2017.
- 1000 Iñiguez, C., Galmés, J., and Gordillo, F. J.: Rubisco carboxylation kinetics and inorganic carbon
1001 utilization in polar versus cold-temperate seaweeds, *J. Exp. Bot.*, 70(4), 1283–1297.
1002 <https://doi.org/10.1093/jxb/ery443>, 2019.
- 1003 Jensen, E. L., Maberly, S. C., and Gontero, B.: Insights on the functions and ecophysiological
1004 relevance of the diverse carbonic anhydrases in microalgae, *Int. J. Mol. Sci.*, 21(8), 2922,
1005 <https://doi.org/10.3390/ijms21082922>, 2020.
- 1006 Johansson, G., and Snoeijs, P.: Macroalgal photosynthetic responses to light in relation to thallus
1007 morphology and depth zonation, *Mar. Ecol. Prog. Ser.*, 244, 63-72, <https://doi:10.3354/meps244063>,
1008 2002.
- 1009 Kim, M. S., Lee, S. M., Kim, H. J., Lee, S. Y., Yoon, S. H., and Shin, K. H.: Carbon stable isotope
1010 ratios of new leaves of *Zostera marina* in the mid-latitude region: implications of seasonal variation
1011 in productivity, *J. Exp. Mar Biol. Ecol.*, 461, 286–296, <https://doi.org/10.1016/j.jembe.2014.08.015>,
1012 2014.
- 1013 Klenell, M., Snoeijs, P., and Pedersen, M.: Active carbon uptake in *Laminaria digitata* and *L.*
1014 *saccharina* (Phaeophyta) is driven by a proton pump in the plasma membrane, *Hydrobiologia*, 514,
1015 41–53, <https://doi.org/10.1023/B:hydr.0000018205.80186.3e>, 2004.
- 1016 Kroopnick, P. M.: The distribution of ^{13}C of ΣCO_2 in the world oceans. *Deep Sea Res. Part I*
1017 *Oceanogr. Res. Pap.*, 32(1), 57-84, [https://doi.org/10.1016/0198-0149\(85\)90017-2](https://doi.org/10.1016/0198-0149(85)90017-2), 1985.
- 1018 Kübler, J. E., and Davison, I. R.: High-temperature tolerance of photosynthesis in the red alga
1019 *Chondrus crispus*, *Mar. Biol.*, 117(2), 327–335. <https://doi.org/10.1007/BF00345678>, 1993.
- 1020 Kübler, J. E., and Dudgeon, S. R.: Predicting effects of ocean acidification and warming on algae

1021 lacking carbon concentrating mechanisms, *PLoS One*, 10 (7),
1022 <https://doi.org/10.1371/journal.pone.0132806>, 2015.

1023 Kübler, J. E., and Raven, J. A.: The interaction between inorganic carbon acquisition and light supply
1024 in *Palmaria palmata* (Rhodophyta), *J. Phycol.*, 31(3), 369-375, [https://doi.org/10.1111/j.0022-](https://doi.org/10.1111/j.0022-3646.1995.00369.x)
1025 [3646.1995.00369.x](https://doi.org/10.1111/j.0022-3646.1995.00369.x), 1995.

1026 Kübler, J. E., and Raven, J. A.: Inorganic carbon acquisition by red seaweeds grown under dynamic
1027 light regimes, *Hydrobiologia*, 326(1), 401-406, 1996.

1028 Lapointe, B. E., and Duke, C. S.: Biochemical strategies for growth of *Gracilaria tikvahiae*
1029 (Rhodophyta) in relation to light intensity and nitrogen availability, *J. Phycol.*, 20(4), 488–495.
1030 <https://doi.org/10.1111/j.0022-3646.1984.00488.x>, 1984.

1031 Littler, M. M., and Littler, D. S.: The evolution of thallus form and survival strategies in benthic
1032 marine macroalgae: field and laboratory tests of a functional form model, *Am Nat.*, 116, 25–44,
1033 1980.

1034 Littler, M. M., and Arnold, K. E.: Primary productivity of marine macroalgal functional-form groups
1035 from south-western North America, *J. Phycol.*, 18, 307–311, [https://doi.org/10.1111/j.1529-](https://doi.org/10.1111/j.1529-8817.1982.tb03188.x)
1036 [8817.1982.tb03188.x](https://doi.org/10.1111/j.1529-8817.1982.tb03188.x), 1982.

1037 Lobban, C. S., Harrison, P. J., and Harrison, P. J.: *Seaweed ecology and physiology*. Cambridge
1038 University Press, 1994.

1039 Lovelock, C. E., Reef, R., Raven, J. A., and Pandolfi, J. M.: Regional variation in $\delta^{13}\text{C}$ of coral reef
1040 macroalgae, *Limnol. Oceanogr.*, <https://doi.org/10.1002/lno.11453>, 2020.

1041 Lluch-Cota, S. E., Aragón-Noriega, E. A., Arreguín-Sánchez, F., Aurióles-Gamboa, D., Bautista-
1042 Romero, J. J., Brusca, R. C., Cervantes-Duarte, R., Cortes-Altamirano, R., Del-MonteLuna, P.,
1043 Esquivel-Herrera, A., Fernández, G., Hendrickx, M. E., Hernandez-Vazquez, S., Herrera-Cervantes,
1044 H., Kahru, M., Lavin, M., Lluch-Belda, D., Lluch-Cota, D. B., López-Martínez, J., Marinone, S. G.,
1045 Nevarez-Martinez, M. O., Ortega-García, S., Palacios-Castro, E., Pares-Sierra, A., Ponce-Díaz, G.,
1046 Ramirez-Rodríguez, M., Salinas-Zavala, C. A., Schwartzlose, R. A., and Sierra-Beltrán, A. P.: The
1047 Gulf of California: Review of ecosystem status and sustainability challenges, *Prog. Oceanogr.*, 73,

- 1048 1–26, <https://doi.org/10.1016/j.pocean.2007.01.013>, 2007.
- 1049 Maberly, S. C., Raven, J. A. and Johnston, A. M.: Discrimination between ^{12}C and ^{13}C by marine
1050 plants, *Oecologia*, 91,481–492, <https://doi.org/10.1007/BF00650320>, 1992.
- 1051 Mackey, A. P., Hyndes, G. A., Carvalho, M. C., and Eyre, B. D.: Physical and biogeochemical
1052 correlates of spatio-temporal variation in the $\delta^{13}\text{C}$ of marine macroalgae, *Estuar. Coast. Shelf Sci.*,
1053 157, 7-18, <https://doi.org/10.1016/j.ecss.2014.12.040>, 2015.
- 1054 Madsen, T. V., and Maberly, S. C.: High internal resistance to CO_2 uptake by submerged
1055 macrophytes that use HCO_3^- : measurements in air, nitrogen and helium, *Photosynth. Res.*, 77(2-3),
1056 183–190, <https://doi.org/10.1023/A:1025813515956>, 2003.
- 1057 Marinone, S. G., and Lavín, M. F.: Residual flow and mixing in the large islands' region of the
1058 central Gulf of California: Nonlinear processes in geophysical fluid dynamics, Springer, Dordrechm,
1059 http://doi-org-443.webvpn.fjmu.edu.cn/10.1007/978-94-010-0074-1_13, 2003.
- 1060 Marinone, S. G.: A note on “Why does the Ballenas Channel have the coldest SST in the Gulf of
1061 California?”. *Geophys. Res. Lett.*, 34(2), <https://doi.org/10.1029/2006GL028589>, 2007.
- 1062 Marconi, M., Giordano, M., and Raven, J. A.: Impact of taxonomy, geography and depth on the $\delta^{13}\text{C}$
1063 and $\delta^{15}\text{N}$ variation in a large collection of macroalgae, *J. Phycol.*, 47, 1023–1035,
1064 <https://doi.org/10.1111/j.1529-8817.2011.01045.x>, 2011.
- 1065 Martínez-Díaz-de-León, A.: Upper-ocean circulation patterns in the Northern Gulf of California,
1066 expressed in Ers-2 synthetic aperture radar imagery, *Cienc. Mar.*, 27(2), 209–221,
1067 <https://doi.org/10.7773/cm.v27i2.465>, 2001.
- 1068 Martínez-Díaz-de-León, A., Pacheco-Ruíz, I., Delgadillo-Hinojosa, F., Zertuche-González, J. A.,
1069 Chee-Barragán, A., Blanco-Betancourt, R., Guzmán-Calderón, J. M., and Gálvez-Telles, A.: Spatial
1070 and temporal variability of the sea surface temperature in the Ballenas-Salsipuedes Channel (central
1071 Gulf of California), *J. Geophys. Res. Oceans*, 111(C2), <https://doi.org/10.1029/2005JC002940>,
1072 2006.
- 1073 Masojidek, J., Kopecká, J., Koblížek, M., and Torzillo, G.: The xanthophyll cycle in green algae

- 1074 (Chlorophyta): its role in the photosynthetic apparatus, *Plant Biol.*, 6(3), 342–349,
1075 <https://doi.org/10.1055/s-2004-820884>, 2004.
- 1076 McConnaughey, T. A., Burdett, J., Whelan, J. F., and Paull, C. K.: Carbon isotopes in biological
1077 carbonates: respiration and photosynthesis, *Geochim. Cosmochim. Ac.*, 61(3), 611–622,
1078 [https://doi.org/10.1016/S0016-7037\(96\)00361-4](https://doi.org/10.1016/S0016-7037(96)00361-4), 1997.
- 1079 Mercado, J. M., De los Santos, C. B., Pérez-Lloréns, J. L., and Vergara, J. J.: Carbon isotopic
1080 fractionation in macroalgae from Cadiz Bay (Southern Spain): comparison with other bio-
1081 geographic regions, *Estuar, Coast. Shelf Sci.*, 85, 449–458,
1082 <https://doi.org/10.1016/j.ecss.2009.09.005>, 2009.
- 1083 Mook, W. G., Bommerson, J. C., and Staverman, W. H.: Carbon isotope fractionation between
1084 dissolved bicarbonate and gaseous carbon dioxide, *Earth Planet. Sci. Lett.*, 22(2), 169–176,
1085 [https://doi.org/10.1016/0012-821X\(74\)90078-8](https://doi.org/10.1016/0012-821X(74)90078-8), 1974.
- 1086 Murru, M., and Sandgren, C.D.: Habitat matters for inorganic carbon acquisition in 38 species of red
1087 macroalgae (Rhodophyta) from Puget Sound, Washington, USA. *J. Phycol.*, 40, 837–845.
1088 <https://doi.org/10.1111/j.1529-8817.2004.03182.x>, 2004.
- 1089 Narvarte, B. C. V., Nelson, W. A., and Roleda, M. Y.: Inorganic carbon utilization of tropical
1090 calcifying macroalgae and the impacts of intensive mariculture-derived coastal acidification on the
1091 physiological performance of the rhodolith *Sporolithon* sp., *Environ. Pollut.*, 266, 115344,
1092 <https://doi.org/10.1016/j.envpol.2020.115344>, 2020.
- 1093 Nielsen, S. L., and Jensen, K. S.: Allometric settling of maximal photosynthetic growth rate to
1094 surface/volume ratio, *Limnol. Oceanogr.*, 35(1), 177–180,
1095 <https://doi.org/10.4319/lo.1990.35.1.0177>, 1990.
- 1096 Norris, J. N.: The marine algae of the northern Gulf of California, Ph. D. dissertation, University of
1097 California, Santa Barbara, 575 pp., 1975.
- 1098 Norris, J. N.: Studies on *Gracilaria* Grev. (Gracilariaceae, Rhodophyta) from the Gulf of California,
1099 Mexico. *Taxonomy of Economic Seaweeds*, California Sea Grant College Program, California, I,
1100 123-135, 1985.

- 1101 Norris, J. N.: Marine algae of the northern Gulf of California: Chlorophyta and Phaeophyceae,
1102 Smithsonian contr. Bot., no. 94, <https://doi.org/10.5479/si.19382812.96>, 2010.
- 1103 Ochoa-Izaguirre, M. J., Aguilar-Rosas, R., and Aguilar-Rosas, L. E.: Catálogo de Macroalgas de las
1104 lagunas costeras de Sinaloa, Serie Lagunas Costeras, Edited by Páez-Osuna, F., UNAM, ICMYL,
1105 México, pp 117, 2007.
- 1106 Ochoa-Izaguirre, M. J., and Soto-Jiménez, M. F.: Variability in nitrogen stable isotope ratios of
1107 macroalgae: consequences for the identification of nitrogen sources, *J. Phycol.*, 51, 46–65,
1108 <https://doi.org/10.1111/jpy.12250>, 2015.
- 1109 Páez-Osuna, F., Piñón-Gimate, A., Ochoa-Izaguirre, M. J., Ruiz-Fernández, A. C., Ramírez-
1110 Reséndiz, G., and Alonso-Rodríguez, R.: Dominance patterns in macroalgal and phytoplankton
1111 biomass under different nutrient loads in subtropical coastal lagoons of the SE Gulf of California,
1112 *Mar. Pollut. Bull.*, 77(1-2), 274-281, <https://doi.org/10.1016/j.marpolbul.2013.09.048>, 2013.
- 1113 Páez-Osuna, F., Álvarez-Borrego, S., Ruiz-Fernández, A. C., García-Hernández, J., Jara-Marini, E.,
1114 Bergés-Tiznado, M. E., Piñón-Gimate, A., Alonso-Rodríguez, R., Soto-Jiménez, M. F., Frías-
1115 Espericueta, M. G., Ruelas-Inzunza, J. R., Green-Ruíz, C. R., Osuna-Martínez, C. C., and Sánchez-
1116 Cabeza, J. A.: Environmental status of the Gulf of California: a pollution review, *Earth-Sci. Rev.*,
1117 166, 181–205, <https://doi.org/10.1016/j.earscirev.2016.09.015>, 2017.
- 1118 Pedroche, F. F., and Senties, A.: Ficología marina mexicana: Diversidad y Problemática actual,
1119 *Hidrobiológica*, 13(1), 23–32, 2003.
- 1120 Quay, P., Sonnerup, R., Westby, T., Stutsman, J., and McNichol, A.: Changes in the $^{13}\text{C}/^{12}\text{C}$ of
1121 dissolved inorganic carbon in the ocean as a tracer of anthropogenic CO_2 uptake, *Glob. Biogeochem.*
1122 *Cycles*, 17(1), 4-1, 2003.
- 1123 Rautenberger, R., Fernández, P. A., Strittmatter, M., Heesch, S., Cornwall, C. E., Hurd, C. L., and
1124 Roleda, M. Y.: Saturating light and not increased carbon dioxide under ocean acidification drive
1125 photosynthesis and growth in *Ulva rigida* (Chlorophyta), *Ecol. Evol.*, 5(4), 874–888,
1126 <https://doi.org/10.1002/ece3.1382>, 2015.
- 1127 Raven, J., Beardall, J., and Griffiths, H.: Inorganic C-sources for *Lemanea*, *Cladophora*, and
1128 *Ranunculus* in a fast-flowing stream: measurements of gas exchange and of carbon isotope ratio and
1129 their ecological implications, *Oecologia*, 53: 68–78, <https://doi:10.1007/BF00377138>., 1982.
- 1130 Raven, J. A., Johnston, A. M., Kübler, J. E., Korb, R. E., McInroy, S. G., Handley, L. L., Scrimgeour,

- 1131 C. M., Walker, D. I., Beardall, J., Clayton, M. N., Vanderklift, M., Fredriksen, S., and Dunton, K.
1132 H.: Seaweeds in cold seas: evolution and carbon acquisition, *Ann. Bot.*, 90, 525–536.
1133 <https://doi.org/10.1093/aob/mcf171>, 2002a.
- 1134 Raven, J. A., Johnsnton, A. M., Kübler, J. E., Korb, R. E., McInroy, S. G., Handley, L. L.,
1135 Scrimgeour, C. M., Walker, D. I., Beardall, J., Vanderklift, M., Fredriksen, S., and Dunton, K. H.:
1136 Mechanistic interpretation of carbon isotope discrimination by marine macroalgae and seagrasses,
1137 *Funct. Plant Biol.*, 29:355–378, <https://doi.org/10.1071/PP01201>, 2002b.
- 1138 Raven, J. A., Ball, L. A., Beardall, J., Giordano, M., and Maberly, S. C.: Algae lacking carbon-
1139 concentrating mechanisms, *Can. J. Bot.*, 83(7), 879–890, <https://doi.org/10.1139/b05-074>, 2005.
- 1140 Raven, J. A., and Beardall, J.: The ins and outs of CO₂, *J. Exp. Bot.*, 67(1), 1–13,
1141 <https://doi.org/10.1093/jxb/erv451>, 2016.
- 1142 Roberts, K., Granum, E., Leegood, R. C., and Raven, J. A.: C₃ and C₄ pathways of photosynthetic
1143 carbon assimilation in marine diatoms are under genetic, not environmental control, *Plant Physiol.*,
1144 145(1), 230–235, <https://doi.org/10.1104/pp.107.102616>, 2007.
- 1145 Robles-Tamayo, C. M., Valdez-Holguín, J. E., García-Morales, R., Figueroa-Preciado, G.,
1146 Herrera-Cervantes, H., López-Martínez, J., and Enríquez-Ocaña, L. F.: Sea surface
1147 temperature (SST) variability of the eastern coastal zone of the gulf of California. *Remote*
1148 *Sensing*, 10(9), 1434, <https://doi.org/10.3390/rs10091434>, 2018.
- 1149 Roden, G. I.: Oceanographic and meteorological aspects of the Gulf of California, *Pac. Sci.*, 12, 21-
1150 45, 1958.
- 1151 Roden, G. I., and Groves, G. W.: Recent oceanographic investigations in the Gulf of California, *J.*
1152 *Mar. Res.*, 18(1), 10–35, 1959.
- 1153 Roden, G. I., and Emilsson, L.: Physical oceanography of the Gulf of California. *Symposium Golfo*
1154 *de California*, Universidad Nacional Autónoma de México, Mazatlán, Sinaloa, México, 1979.
- 1155 Roleda, M. Y., Boyd, P. W., and Hurd, C. L.: Before ocean acidification: calcifier chemistry lessons,
1156 *J. Phycol.*, 48(4), 840-843, 2012.
- 1157 Roleda, M. Y., and Hurd, C. L.: Seaweed responses to ocean acidification, in: *Seaweed biology*

- 1158 (Novel Insights into Ecophysiology, Ecology and Utilization), edited by: Caldwell, M. M.,
1159 Heldmaier, G., Jackson, R. B., Lange, O. L., Mooney, H. A., Schulze, E.-D., and Sommer, U.,
1160 Springer, Berlin, Heidelberg, 407-431, 2012.
- 1161 Rusnak, G. A., Fisher, R. L., and Shepard, F. P.: Bathymetry and faults of Gulf of California. In: van
1162 An del, Tj. H. and G.G. Shor, Jr. (editors), Marine Geology of the Gulf of California: A symposium,
1163 AAPG Memoir, 3, 59–75, <https://doi.org/10.1306/M3359C3>, 1964.
- 1164 Sand-Jensen, K., and Gordon, D.: Differential ability of marine and freshwater macrophytes to utilize
1165 HCO_3^- and CO_2 , *Mar. Biol.*, 80, 247–253, <https://doi.org/10.1111/j.1469-8137.1981.tb03198.x>,
1166 1984.
- 1167 Sanford, L. P., and Crawford, S. M.: Mass transfer versus kinetic control of uptake across solid-
1168 water boundaries, *Limnol. Oceanogr.*, 45, 1180–1186, <https://doi.org/10.4319/lo.2000.45.5.1180>,
1169 2000.
- 1170 Santamaría-del-Angel, E., Alvarez-Borrego, S., and Müller-Karger, F. E.: Gulf of California
1171 biogeographic regions based on coastal zone color scanner imagery, *J. Geophys. Res.*, 99,
1172 7411–7421, <https://doi.org/10.1029/93JC02154>, 1994.
- 1173 Santos, G. M., Ferguson, J., Acaylar, K., Johnson, K. R., Griffin, S., and Druffel, E.: $\Delta^{14}\text{C}$ and $\delta^{13}\text{C}$
1174 of seawater DIC as tracers of coastal upwelling: A 5-year time series from Southern California,
1175 *Radiocarbon*, 53(4), 669-677, <https://doi.org/10.1017/S0033822200039126>, 2011.
- 1176 Setchell, W., and Gardner, N.: The marine algae of the Pacific Coast of North America. Part II
1177 Chlorophyceae, *Univ. Calif. Publ. Bot.*, 8, 139–374, <https://doi.org/10.5962/bhl.title.5719>, 1920.
- 1178 Setchell, W., and Gardner, N.: The marine algae: Expedition of the California Academy of Sciences
1179 to the Gulf of California in 1921, *Proc. Calif. Acad. Sci.*, 4th series, 12(29), 695–949, 1924.
- 1180 Sharkey, T. D., and Berry, J. A.: Carbon isotope fractionation of algae as influenced by an inducible
1181 CO_2 concentrating mechanism. Inorganic carbon uptake by aquatic photosynthetic organisms, 389-
1182 401, 1985.
- 1183 Stepien, C. C.: Impacts of geography, taxonomy and functional group on inorganic carbon use
1184 patterns in marine macrophytes, *J. Ecol.*, 103(6), 1372–1383, <https://doi.org/10.1111/1365-2745.12451>, 2015.

- 1186 Stroup, W. W., Milliken, G. A., Claassen, E. A., & Wolfinger, R. D. (2018). SAS for mixed models:
1187 introduction and basic applications. SAS Institute.
- 1188 Teichberg, M., Fox, S. E., Olsen, Y. S., Valiela, I., Martinetto, P., Iribarne, O., Muto, E. Y., Petti,
1189 M. A., Cobrisier, T. N., Soto-Jiménez, M., Páez-Osuna, F., Castro, P., Freitas, H., Zitelli, A.,
1190 Cardinaletti, M. and Tagliapietra, D.: Eutrophication and macroalgal blooms in temperate and
1191 tropical coastal waters: nutrient enrichment experiments with *Ulva* spp., *Glob. Chang. Biol.*, 16(9),
1192 2624-2637, <https://doi.org/10.1111/j.1365-2486.2009.02108.x>, 2010.
- 1193 Valiela, I., Liu, D., Lloret, J., Chenoweth, K., and Hanacek, D.: Stable isotopic evidence of
1194 nitrogen sources and C4 metabolism driving the world's largest macroalgal green tides in the
1195 Yellow Sea, *Sci. Rep.*, 8(1), 1–12, <https://doi.org/10.1038/s41598-018-35309-3>, 2018.
- 1196 Vásquez-Elizondo, R. M., and Enríquez, S.: Light absorption in coralline algae (Rhodophyta): a
1197 morphological and functional approach to understanding species distribution in a coral reef lagoon,
1198 *Front. Mar. Sci.*, 4, 297, <https://doi.org/10.3389/fmars.2017.00297>, 2017.
- 1199 Vásquez-Elizondo, R. M., Legaria-Moreno, Pérez-Castro, M.A., Krämer, W. E., Scheufen, T.,
1200 Iglesias-Prieto, R., and Enríquez, S.: Absorptance determinations on multicellular tissues,
1201 *Photosynth. Res.*, 132, 311–324, <https://doi.org/10.1007/s11120-017-0395-6>, 2017.
- 1202 Velasco-Fuentes, O. V., and Marinone, S. G.: A numerical study of the Lagrangian circulation in the
1203 Gulf of California, *J. Mar. Syst.*, 22(1), 1–12. [https://doi.org/10.1016/S0924-7963\(98\)00097-9](https://doi.org/10.1016/S0924-7963(98)00097-9),
1204 1999.
- 1205 Young, E. B., and Beardall, J.: Modulation of photosynthesis and inorganic carbon acquisition in a
1206 marine microalga by nitrogen, iron, and light availability, *Can. J. Bot.*, 83(7), 917–928,
1207 <https://doi.org/10.1139/b05-081>, 2005.
- 1208 Young, J. N., Heureux, A. M., Sharwood, R. E., Rickaby, R. E., Morel, F. M., and Whitney, S. M.:
1209 Large variation in the Rubisco kinetics of diatoms reveals diversity among their carbon-
1210 concentrating mechanisms, *J. Exp. Bot.*, 67(11), 3445–3456, <https://doi.org/10.1093/jxb/erw163>,
1211 2016.
- 1212 Xu, J., Fan, X., Zhang, X., Xu, D., Mou, S., Cao, S., Zheng, Z., Miao, J., Ye, N.: Evidence of
1213 coexistence of C3 and C4 photosynthetic pathways in a green-tide-forming alga, *Ulva prolifera*, *PloS*

- 1214 one, 7(5), e37438, <https://doi.org/10.1371/journal.pone.0037438>, 2012.
- 1215 Xu, J., Zhang, X., Ye, N., Zheng, Z., Mou, S., Dong, M., Xu, D. and Miao, J.: Activities of principal
1216 photosynthetic enzymes in green macroalga *Ulva linza*: functional implication of C4 pathway in CO₂
1217 assimilation, *Sci. China Life Sci.*, 56(6), 571–580, <https://doi.org/10.1007/s11427-013-4489-x>,
1218 2013.
- 1219 Wiencke, C., and Fischer, G.: Growth and stable carbon isotope composition of cold-water
1220 macroalgae in relation to light and temperature, *Mar. Ecol Prog. Ser.*, 283-292, 1990.
- 1221 Wilkinson, T. E., Wiken, J., Bezaury-Creel, T., Hourigan, T., Agardy, H., Herrmann, L., Janishevski,
1222 C. Madden, L. Morgan and M. Padilla.: *Marine Ecoregions of North America*. CEC, Montreal,
1223 Canada, 2009.
- 1224 Zabaleta, E., Martin, M. V., and Braun, H. P.: A basal carbon concentrating mechanism in plants?,
1225 *Plant Sci.*, 187, 97–104, <https://doi.org/10.1016/j.plantsci.2012.02.001>, 2012.
- 1226 Zeebe, R. E., and Wolf-Gladrow, D.: *CO₂ in seawater: equilibrium, kinetics, isotopes* (No. 65) Gulf
1227 Professional Publishing, 2001.
- 1228 Zeitzschel, B.: Primary productivity in the Gulf of California, *Mar. Biol.*, 3(3), 201–207,
1229 <https://doi.org/10.1007/BF00360952>, 1969.
- 1230 Zou, D., Xia, J., and Yang, Y.: Photosynthetic use of exogenous inorganic carbon in the agarophyte
1231 *Gracilaria lemaneiformis* (Rhodophyta), *Aquac.*, 237, 421-431,
1232 <https://doi.org/10.1016/j.aquaculture.2004.04.020>, 2004.
- 1233

1234 **Figure captions**

1235 Fig. 1. Sites collection along the continental (C1-C3) and peninsula (P1-P3) Gulf of California
1236 coastlines (A), range of environmental factors supporting or limiting the life processes for the
1237 macroalgal communities within a habitat (B), and inserted Table with the features and
1238 environmental conditions in the diverse habitats in the GC bioregions that delimits the macroalgal
1239 community's zonation.

1240 Fig. 2. Variability of $\delta^{13}\text{C}$ values for specimens of different macroalgae genera collected along GC
1241 coastlines classified by taxon: (A) Chlorophyta, (B) Ochrophyta and (C) Rhodophyta. Shaded
1242 background represents the cutoff limits for using CO_2 Only users and HCO_3^- only users,
1243 respectively, according to Raven et al. (2002).

1244 Fig. 3. Variability of $\delta^{13}\text{C}$ values for the genus collected along coastline of the Gulf of California
1245 according to their taxon: (A) Chlorophyta, (B) Ochrophyta and (C) Rhodophyta. Genus with n=1 is
1246 not shown, and genus n=2 was not considered to the statistical comparison. Different letters
1247 indicate significant differences ($P < 0.05$): a>b>c>d>e. Shaded background represent the cutoff
1248 limits for using CO_2 Only users and HCO_3^- only users, respectively, according to Raven et al.,
1249 (2002). For Chlorophyta: Bry= *Bryopsis*, Cau= *Caulerpa*, Cha= *Chaetomorpha*, Cla= *Cladophora*,
1250 Cod= *Codium*, Phy= *Phyllocladon*, Str= *Struveopsis*, Ulv= *Ulva*. Phaeophyta: Col= *Colpomenia*,
1251 Dic= *Dictyota*, Ect= *Ectocarpus*, End= *Endarachne*, Hyd= *Hydroclathrus*, Pad= *Padina*, Ros=
1252 *Rosenvingea*, Sar= *Sargassum*, Spa= *Spatoglossum*, Zon= *zonaria*. Rhodophyta: Aca:
1253 *Acantophora*, anf: *Anfeltiopsis*, Amp= *Amphiroa*, Cen= *Centroceras*, Cer¹= *Ceramium*, Cer²=
1254 *Ceratodictyon*, Cho¹= *Chondracanthus*, Cho²= *Chondria*, Das= *Dasya*, Dig= *Digenia*, Euc=
1255 *Euchema*, Gel= *Gelidium*, Gig= *Gigartina*, Gra¹= *Gracilaria*, Gra²= *Grateloupia*, Gra³=

1256 *Gracilariopsis*, Gym= *Gymnogongrus*, Hal= *Halymenia*, Hyp= *Hypnea*, Jan= *Jania*, Lau=
1257 *Laurencia*, Lom= *Lomentaria*, Neo= *Neosiphonia*, Pol= *Polysiphonia*, Pri= *Prionitis*, Rho¹=
1258 *Rhodoglossum*, Rho²= *Rhodymenia*, Sch= *Schizymenia*, Spy= *Spyridia*, Tac= *Tacanoosca*.

1259 Fig. 4. Variability of $\delta^{13}\text{C}$ values for morphofunctional groups by taxa along coastline of the Gulf
1260 of California.

1261 Fig. 5 Proportion of species using different DIC sources according to their carbon uptake
1262 strategies: HCO_3^- only users (CO_2 concentrating mechanism active), Users of both sources (HCO_3^-
1263 & CO_2) and CO_2 only users (non- CO_2 concentrating mechanism active) in function of coast along
1264 GC.

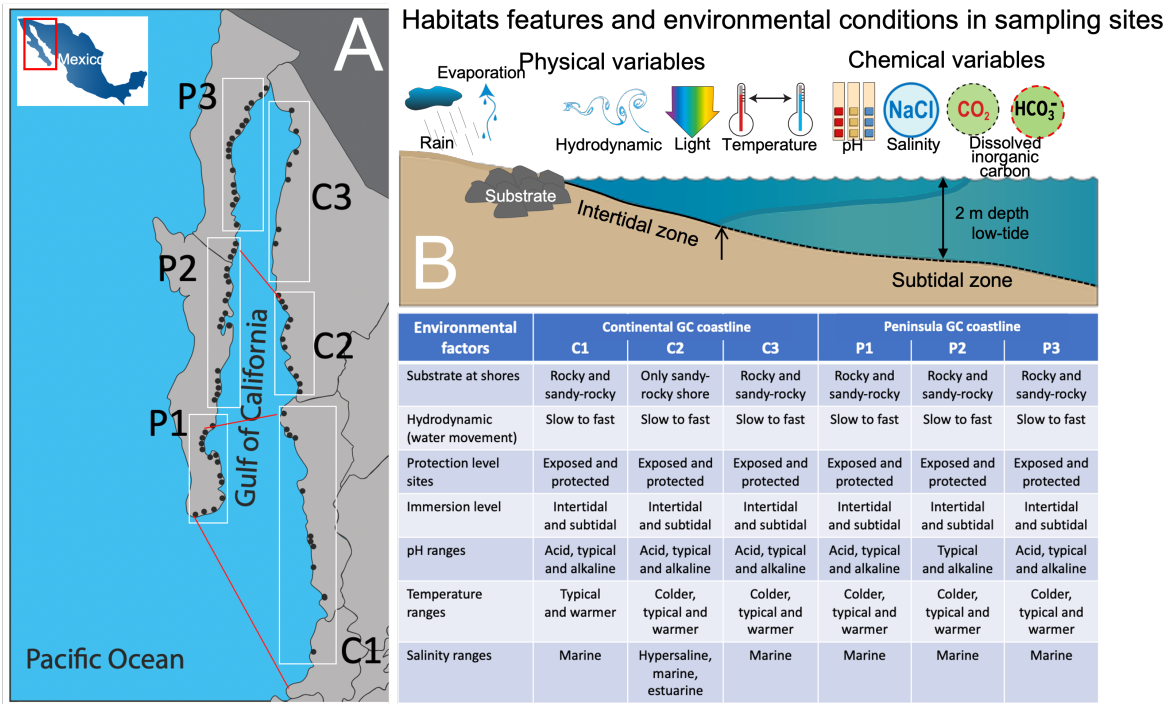
1265 Fig. 6. Variability of $\delta^{13}\text{C}$ values in macroalgae specimens for the most representative genera in
1266 function of habitat features (emersion level). Green circles represent genus of Chlorophyta, Brown
1267 circles represent genus of Ochrophyta; red circles represent genus Rhodophyta.

1268 Fig. 7. Variability of $\delta^{13}\text{C}$ values in macroalgae specimens for the most representative genus in
1269 function of temperature (a) and pH (b) ranges in samples collected along Gulf of California
1270 coastline.

1271 Fig. 8. Proportion of species using different DIC sources according to their carbon assimilation
1272 strategies: HCO_3^- only users (CO_2 concentrating mechanism active), Users of both sources (HCO_3^-
1273 & CO_2) and CO_2 only users (non- CO_2 concentrating mechanism active) in function of : (A) pH
1274 ranges, (B) temperature ranges and (C) salinity ranges.

1275 Fig. 9. Trends in the $\delta^{13}\text{C}$ -macroalgal in specimens collected along continental (C1-C3) and
1276 peninsula (P1-P3) Gulf of California coastline in function of latitudinal gradient.

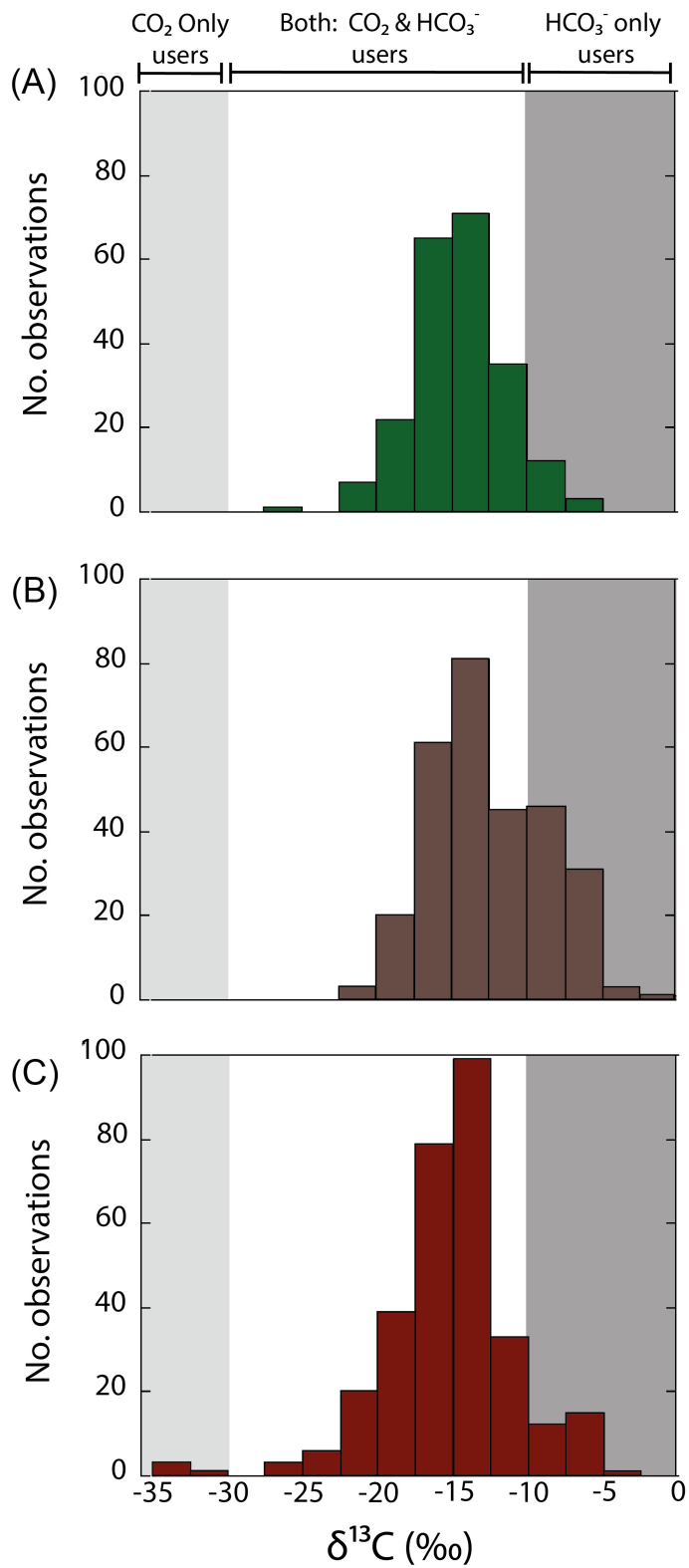
1277



1278

1279 Fig. 1

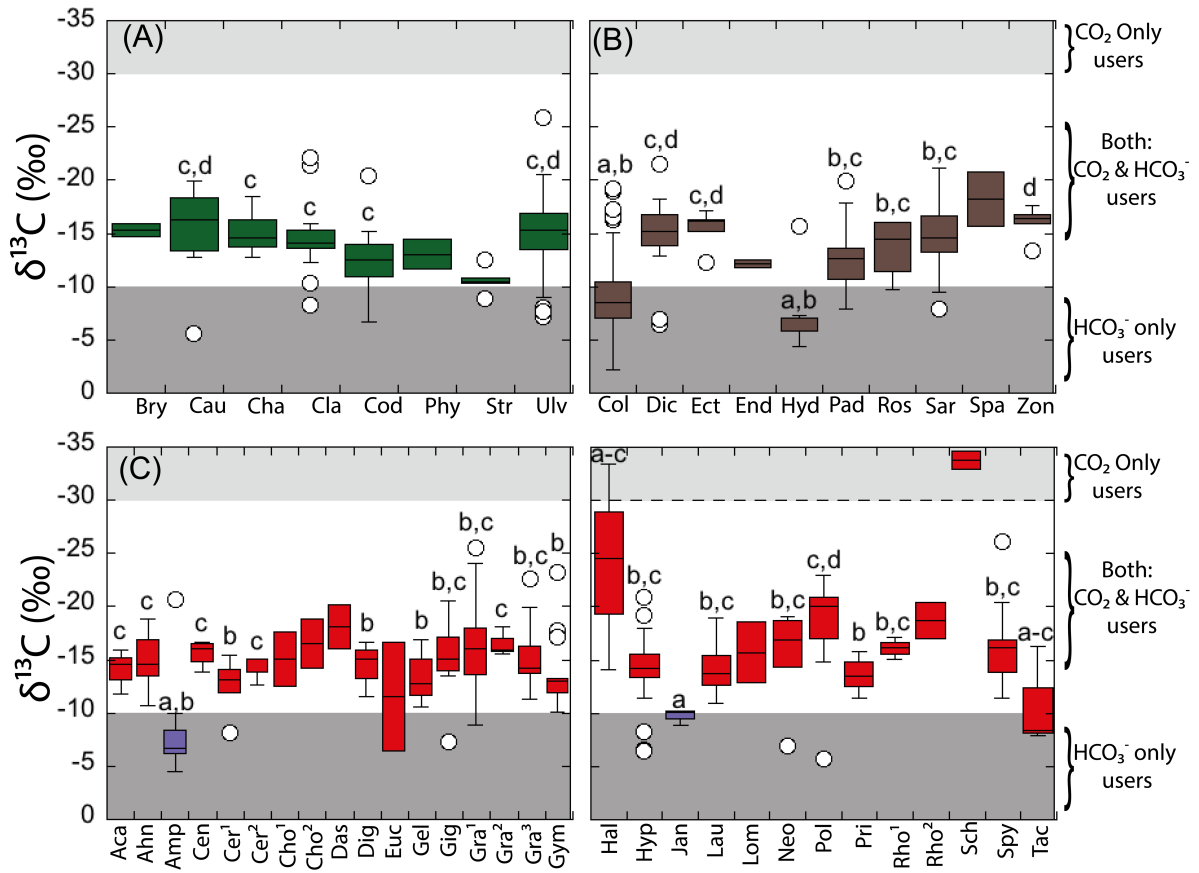
1280



1281

1282 Fig. 2

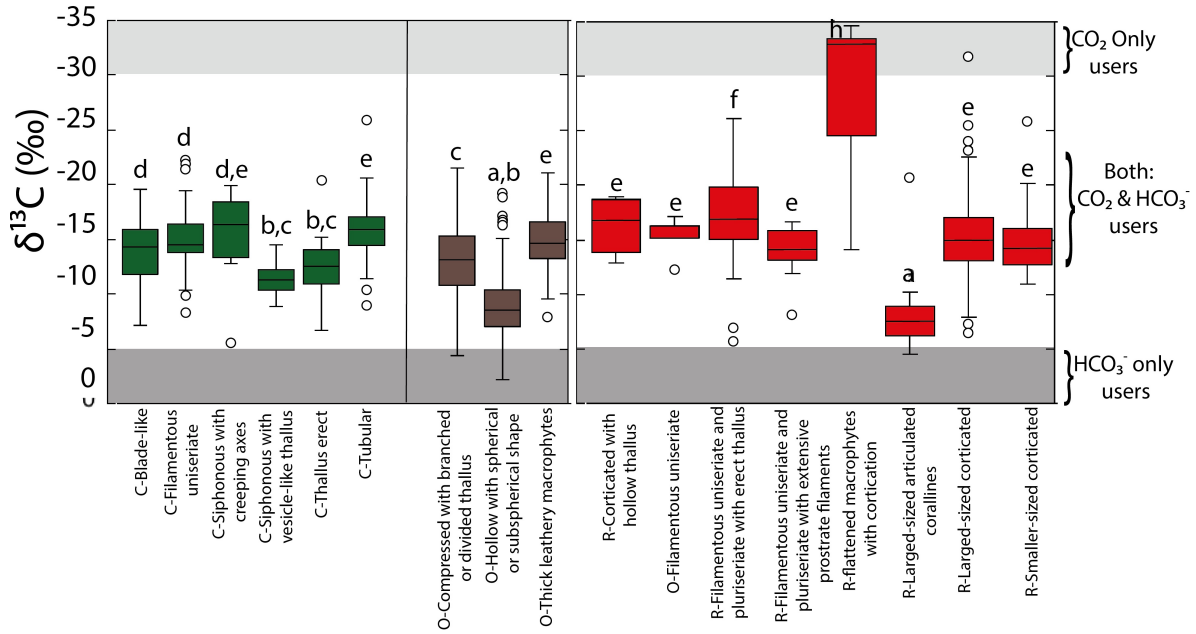
1283



1284

1285 Fig. 3

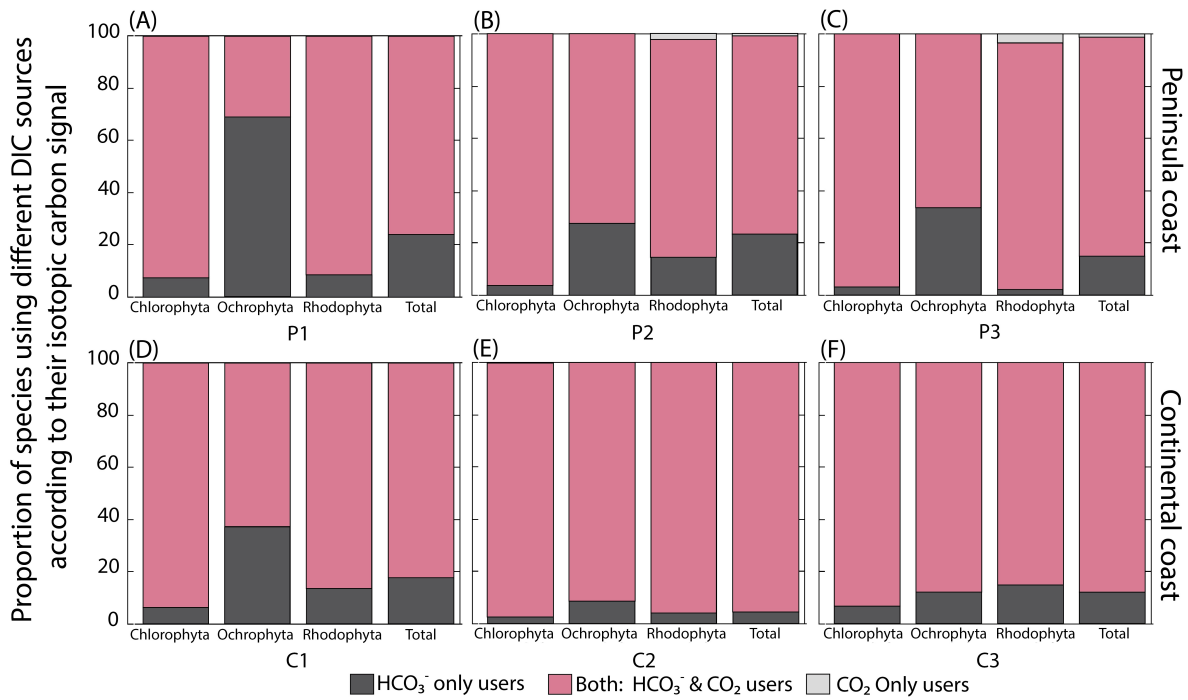
1286



1287

1288 Fig. 4

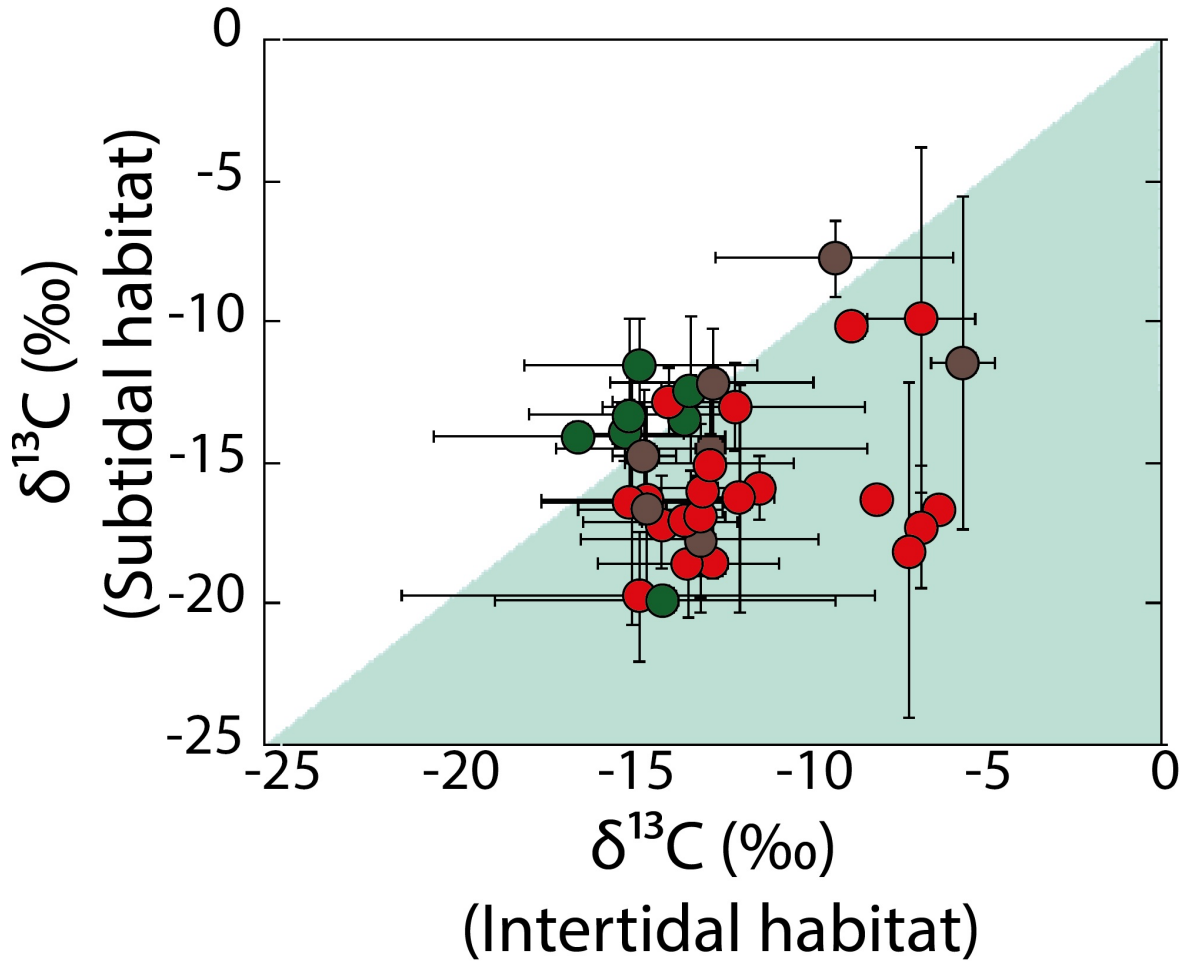
1289



1290

1291 Fig. 5

1292

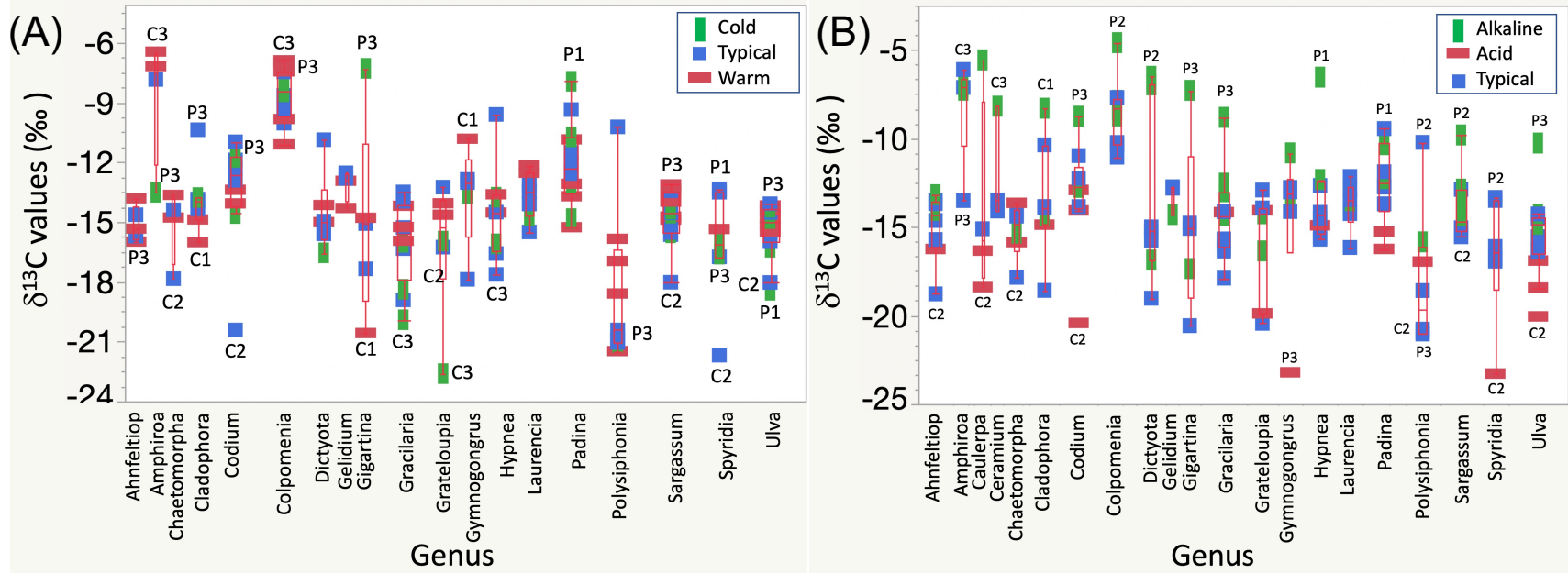


1293

1294 Fig. 6

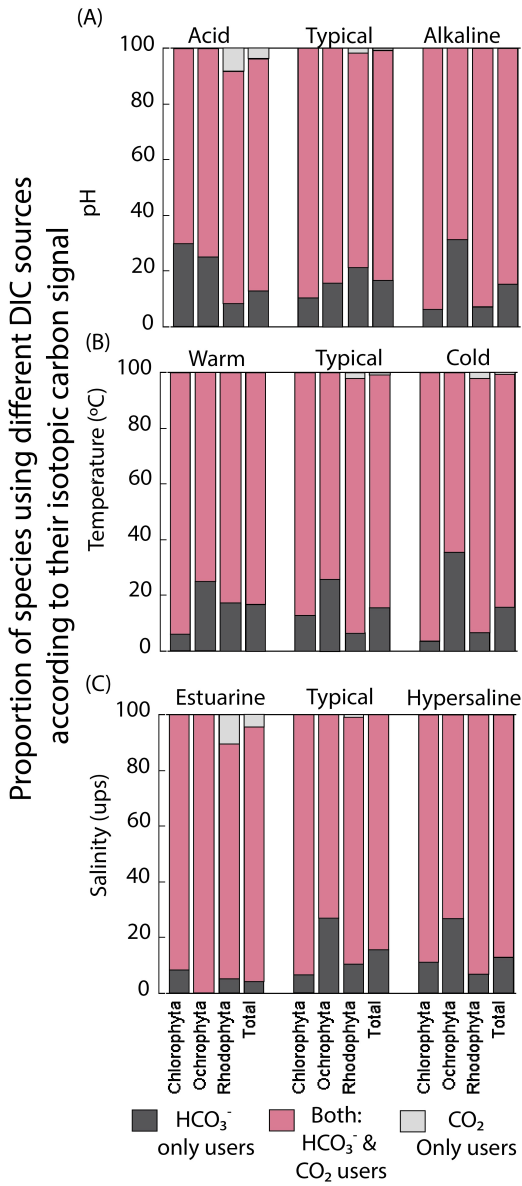
1295

1296



1297

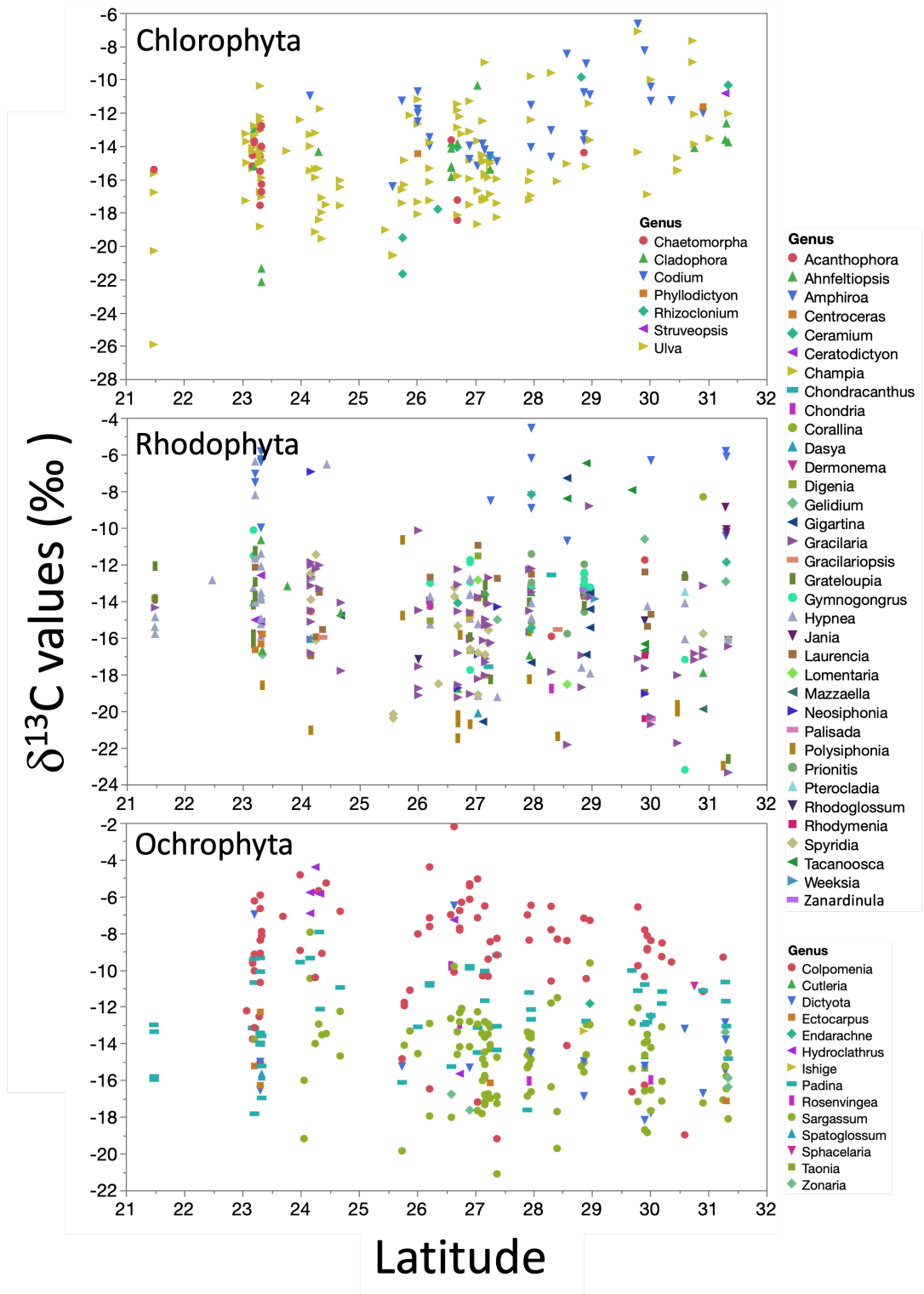
1298 **Fig 7**



1300

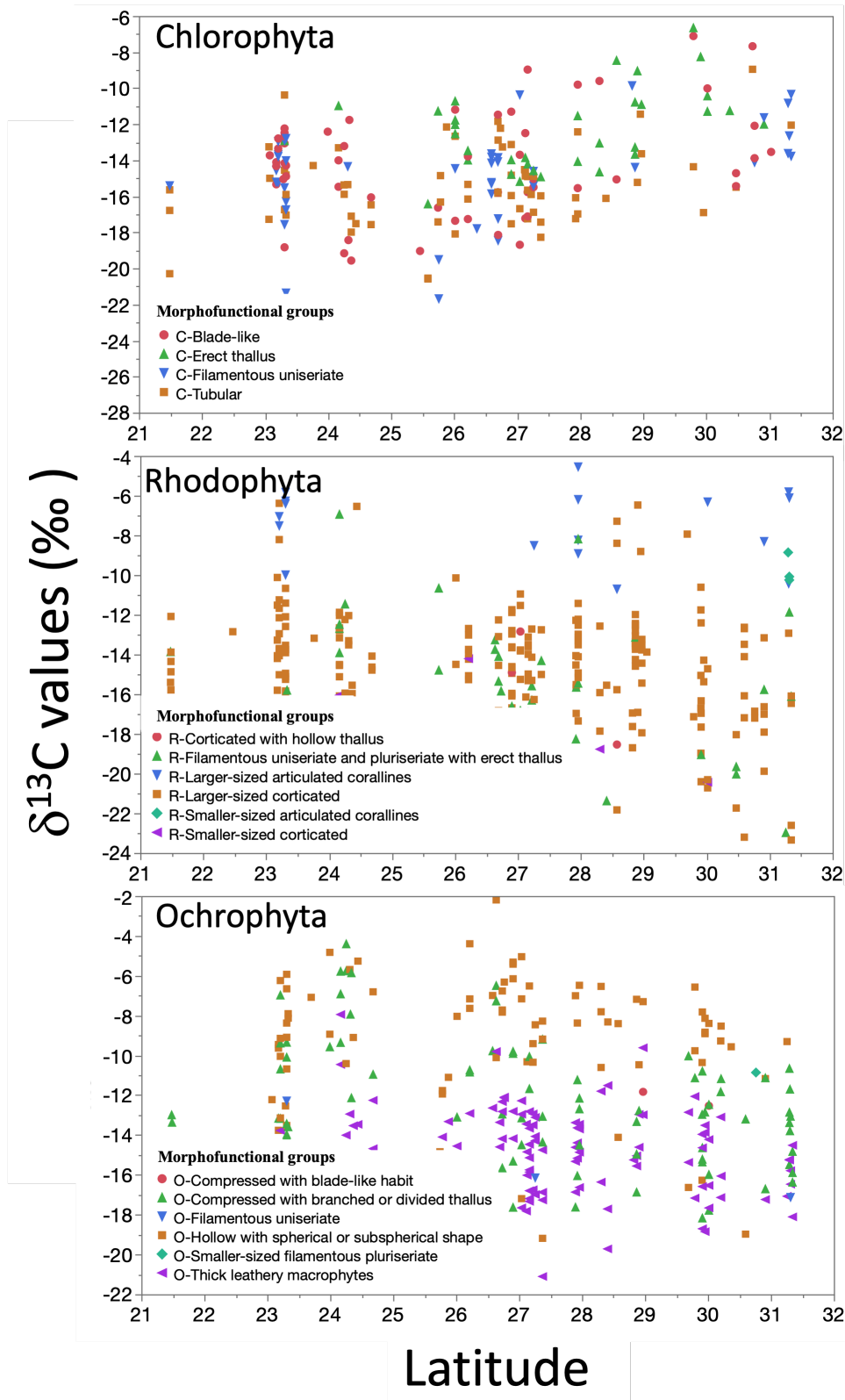
1301 Fig. 8

1302



1303

1304 Fig. 9



1305

1306 Fig. 10

Table 1. Carbon isotopic composition (‰) in species of Phylum Chlorophyta collected along Gulf of California coastlines.

Species (n composite samples)	$\delta^{13}\text{C} \pm \text{SD}$ (Min to Max, ‰)
<i>Chaetomorpha</i> sp. (3)	-13.7 \pm 0.8 (-14.6 to -12.9)
<i>C. antennina</i> (10)	-14.6 \pm 1.1 (-16.3 to -12.8)
<i>C. linum</i> (5)	-16.8 \pm 1.6 (-18.4 to -14.6)
<i>Codium</i> sp. (5)	-11.6 \pm 3.0 (-14.1 to -6.7)
<i>C. amplivesiculatum</i> (8)	-14.4 \pm 2.7 (-20.4 to -11.3)
<i>C. brandegeei</i> (7)	-11.8 \pm 1.2 (-13.7 to -10.4)
<i>C. fragile</i> (4)	-13.0 \pm 2.7 (-14.8 to -9.0)
<i>C. simulans</i> (9)	-11.4 \pm 2.2 (-14.9 to -8.3)
<i>Ulva</i> sp. (12)	-14.0 \pm 3.9 (-19.2 to -7.1)
<i>U. acanthophora</i> (25)	-15.8 \pm 1.7 (-18.3 to -11.4)
<i>U. clathrata</i> (8)	-16.4 \pm 2.0 (-20.5 to -14.5)
<i>U. compressa</i> (4)	-17.8 \pm 2.4 (-20.6 to -15.4)
<i>U. flexuosa</i> (13)	-16.0 \pm 3.7 (-25.9 to -10.4)
<i>U. intestinalis</i> (16)	-15.3 \pm 2.5 (-20.3 to -8.9)
<i>U. lactuca</i> (31)	-14.1 \pm 3.1 (-19.6 to -7.7)
<i>U. linza</i> (6)	-15.6 \pm 2.4 (-19.4 to -13.2)
<i>U. lobata</i> (5)	-13.2 \pm 1.9 (-15.3 to -11.1)
<i>U. prolifera</i> (3)	-14.2 \pm 1.8 (-15.5 to -12.2)

Table 2. Carbon isotopic composition (‰) in species of Phylum Ochrophyta collected along Gulf of California coastlines.

Species (n composite samples)	$\delta^{13}\text{C} \pm \text{SD}$ (Min to Max, ‰)
<i>Colpomenia</i> sp. (11)	-11.0 \pm 3.7 (-19.0 to -5.4)
<i>C. ramosa</i> (4)	-11.4 \pm 2.6 (-13.8 to -7.8)
<i>C. sinuosa</i> (7)	-10.2 \pm 3.0 (-16.3 to -7.2)
<i>C. tuberculata</i> (64)	-8.7 \pm 3.2 (-19.2 to -2.2)
<i>Padina</i> sp. (15)	-11.1 \pm 1.5 (-13.1 to -7.9)
<i>P. crispata</i> (3)	-11.3 \pm 1.7 (-12.5 to -10.1)
<i>P. durvillei</i> (36)	-13.2 \pm 2.6 (-20.0 to -9.2)
<i>Sargassum</i> sp. (34)	-14.3 \pm 2.4 (-18.7 to -8.0)
<i>S. herporhizum</i> (7)	-13.7 \pm 1.6 (-16.6 to -11.5)
<i>S. horridum</i> (12)	-15.5 \pm 2.9 (-19.7 to -9.5)
<i>S. johnstonii</i> (10)	-15.4 \pm 2.0 (-17.7 to -11.8)
<i>S. lapazeanum</i> (7)	-14.5 \pm 1.6 (-17.2 to -12.8)
<i>S. sinicola</i> (31)	-15.1 \pm 2.4 (-21.1 to -12.1)

1308

1309 Table 3. Carbon isotopic composition (‰) in species of Phylum Rhodophyta collected along Gulf
 1310 of California coastlines.

Species (n composite samples)	$\delta^{13}\text{C} \pm \text{SD}$ (Min to Max, ‰)
<i>Gracilaria</i> sp. (18)	-15.5 \pm 2.4 (-21.8 to -12.2)
<i>Gracilaria</i> sp.2 (3)	-14.4 \pm 3.7 (-18.7 to -12.3)
<i>G. crispata</i> (7)	-15.1 \pm 3.0 (-19.1 to -10.1)
<i>G. pacifica</i> (6)	-16.5 \pm 1.6 (-18.6 to -13.6)
<i>G. spinigera</i> (3)	-14.9 \pm 3.8 (-17.7 to -12.2)
<i>G. subsecundata</i> (8)	-15.9 \pm 2.8 (-20.3 to -12.8)
<i>G. tepocensis</i> (3)	-15.1 \pm 1.9 (-17.0 to -13.2)
<i>G. textorii</i> (4)	-16.2 \pm 2.6 (-18.1 to -14.3)
<i>G. turgida</i> (5)	-15.3 \pm 3.6 (-20.7 to -12.0)
<i>G. vermiculophylla</i> (16)	-15.9 \pm 3.8 (-23.4 to -8.8)
<i>Hypnea</i> sp. (14)	-14.9 \pm 2.6 (-20.9 to -11.4)
<i>H. johnstonii</i> (5)	-11.2 \pm 3.5 (-13.8 to -6.5)
<i>H. pannosa</i> (5)	-11.8 \pm 3.3 (-15.0 to -6.4)
<i>H. spinella</i> (6)	-16.4 \pm 1.8 (-19.2 to -14.9)
<i>H. valentiae</i> (6)	-15.2 \pm 2.3 (-19.2 to -12.7)
<i>Laurencia</i> sp. (8)	-12.9 \pm 1.2 (-14.7 to -10.5)
<i>L. pacifica</i> (8)	-14.9 \pm 2.2 (-19.0 to -12.7)
<i>L. papillosa</i> (3)	-15.7 \pm 0.3 (-15.9 to -15.6)
<i>Spyrida</i> sp. (5)	-17.1 \pm 1.12 (-19.1 to -16.1)
<i>S. filamentosa</i> (14)	-15.9 \pm 3.8 (-26.2 to -11.5)

1311

1312

1313

1314 Table 4. Summary of the estimated regression coefficients for each simple linear regression
 1315 analyses and on the constant of fitted regression models. Estimated regression coefficients includes
 1316 degrees of freedom for the error (DFE), root-mean-square error (RMSE), coefficients of
 1317 determination (R^2) and the adjusted R^2 statistics, Mallow's Cp criterion (Cp), Akaike Information
 1318 Criterion (AIC), Bayesian Information Criterion (BIC) minimum, F Ratio test, and p-value for the
 1319 test (Prob > F). Models information includes value of the constant a ($\delta^{13}C$, ‰), standard error (SE),
 1320 t ratio and Prob > |t| (values * are significant).

Independent variables	Estimated regression coefficients								Model constant (a)				
	DFE	RMSE	R^2	Adjust R^2	Cp	AICc	BIC	F ratio	Prob > F	$\delta^{13}C$ (‰)	SE	t ratio	Prob > t
Inherent macroalgae properties													
Phyla	806	3.66	0.08	0.07	3	4,401	4,420	33.1	<.0001**	-13.98	0.13	-107.4	<.0001**
Morphofunctional	788	3.10	0.35	0.34	21	4,149	4,251	21.6	<.0001**	-14.21	0.35	-40.80	<.0001**
Genus	746	2.92	0.46	0.41	63	4,104	4,393	10.1	<.0001**	-14.71	0.23	-62.64	<.0001*
Species	641	2.79	0.57	0.46	168	4,195	4,898	5.2	<.0001**	-14.60	0.16	-93.22	<.0001**
Biogeographical collection zone													
GC coastline	807	3.79	0.01	0.01	2	4,456	4,470	7.4	0.0067*	-13.97	0.13	-104.5	<.0001**
Coastal sector	803	3.73	0.05	0.04	6	4,433	4,465	7.9	<.0001*	-14.12	0.16	-90.85	<.0001**
Latitude	807	3.80	0.00	0.00	2	4,462	4,476	1.5	0.23	-12.25	1.41	-8.71	<.0001**
Longitude	807	3.81	0.00	0.00	2	4,463	4,477	0.1	0.80	-15.44	5.83	-2.65	0.0082*
Habitat features													
Substrate	807	3.80	0.00	0.00	2	4,460	4,474	3.2	0.08	-13.82	0.15	-92.06	<.0001*
Hydrodynamic	807	3.80	0.00	0.00	2	4,462	4,476	1.3	0.26	-13.88	0.15	-95.00	<.0001**
Emersion level	807	3.69	0.06	0.06	2	4,412	4,427	52.2	<.0001**	-14.05	0.13	-107.6	<.0001**
Environmental conditions													
Temperature	802	3.70	0.01	0.01	2	4,390	4,404	5.4	0.0207*	-16.11	0.96	-16.78	<.0001*
pH	807	3.73	0.04	0.04	2	4,430	4,444	33.4	<.0001**	-32.45	3.21	-10.13	<.0001**
Salinity	806	3.80	0.00	0.00	2	4,456	4,470	0.9	0.34	-15.77	1.91	-8.27	<.0001**

1321 *p<0.05, **p<0.0001

1322 Table 5. Summary of the estimated regression coefficients for each multivariate linear
 1323 regression analyses and on their constant of fitted regression models performed in
 1324 individuals binned by genus. Estimated regression coefficients include degrees of freedom
 1325 for the error (DFE), root-mean-square error (RMSE), coefficients of determination (R^2) and
 1326 the adjusted R^2 statistics, Mallows' Cp criterion (Cp), Akaike Information Criterion (AIC),
 1327 Bayesian Information Criterion (BIC) minimum, F Ratio test, and p-value for the test (Prob
 1328 > F). Model information includes value of the constant a ($\delta^{13}C$, ‰), standard error (SE), t
 1329 ratio and Prob > |t| (values * are significant).

Independent variables	Estimated regression coefficients								Model constant (a)				
	DFE	RMSE	R^2	Adjust R^2	Cp	AICc	BIC	F ratio	Prob > F	$\delta^{13}C$ (‰)	SE	t ratio	Prob > t
Coastal sector	652	2.78	0.57	0.47	157	4,169	4,834	20.0	<.0001*	-17.52	0.64	-27.24	<.0001*
Substrate	711	2.90	0.49	0.42	98	4,140	4,577	0.4	0.52	-16.35	0.62	-26.20	<.0001*
Hydrodynamic	714	2.87	0.50	0.43	95	4,120	4,545	0.1	0.78	-16.53	0.64	-25.95	<.0001*
Emersion level	713	2.77	0.53	0.47	96	4,060	4,489	153.0	<.0001*	-16.65	0.60	-27.85	<.0001*
Temperature	695	2.81	0.50	0.43	109	4,083	4,564	98.4	<.0001*	-14.60	0.92	-15.91	<.0001*
Temperature ranges	686	2.87	0.49	0.40	118	4,128	4,645	97.7	<.0001*	-12.91	0.40	-31.97	<.0001*
pH	701	2.86	0.51	0.43	108	4,134	4,611	156.6	<.0001*	-28.57	2.69	-10.64	<.0001*
pH ranges	697	2.67	0.57	0.51	112	4,028	4,522	152.2	<.0001*	-16.39	0.58	-28.05	<.0001*
Salinity	697	2.89	0.50	0.42	111	4,151	4,640	162.2	<.0001*	-17.75	1.63	-10.88	<.0001*
Salinity ranges	721	2.91	0.47	0.41	86	4,117	4,504	167.8	<.0001*	-17.64	0.74	-23.68	<.0001*

1330

1331

1332

1333

1334

1335

1336 Table 6. Summary of the estimated regression coefficients for each multivariate linear regression
 1337 analyses and on their constant of fitted regression models performed in individuals binned by
 1338 coastline sector and genus. Estimated regression coefficients include degrees of freedom for the
 1339 error (DFE), root-mean-square error (RMSE), coefficients of determination (R^2) and the adjusted
 1340 R^2 statistics, Mallows' Cp criterion (Cp), Akaike Information Criterion (AIC), Bayesian
 1341 Information Criterion (BIC) minimum, F Ratio test, and p-value for the test (Prob > F). Model
 1342 information includes value of the constant a ($\delta^{13}C$, ‰), standard error (SE), t ratio and Prob > |t|
 1343 (values * are significant).

Independent variables	DFE	RMSE	Estimated regression coefficients						Prob > F	Model constant (a)			
			R ²	Adjust R ²	Cp	AICc	BIC	F ratio		$\delta^{13}C$ (‰)	SE	t ratio	Prob > t
Substrate	590	2.76	0.62	0.47	219	4,287	5,155	15.8	<.0001*	-17.08	0.66	-25.72	<.0001*
Hydrodynamic	592	2.73	0.62	0.49	217	4,266	5,128	18.6	<.0001*	-17.18	0.67	-25.70	<.0001*
Protection level	590	2.75	0.62	0.48	219	4,285	5,153	20.0	<.0001*	-17.51	0.64	-27.22	<.0001*
Emersion level	603	2.69	0.63	0.50	206	4,217	5,045	18.6	<.0001*	-17.47	0.64	-27.49	<.0001*
Temperature ranges	569	2.74	0.61	0.46	235	4,293	5,202	28.0	<.0001*	-13.73	0.45	-30.32	<.0001*
pH ranges	580	2.50	0.69	0.57	229	4,155	5,051	9.7	0.0019*	-16.88	0.62	-27.15	<.0001*
Salinity ranges	631	2.76	0.58	0.47	176	4,183	4,913	21.2	<.0001*	-18.30	0.79	-23.05	<.0001*

1344

1345

1346 Table 7. Summary of the estimated regression coefficients for each multivariate linear regression
 1347 analyses and on their constant of fitted regression models performed in individuals binned in
 1348 coastline sector, habitats features, environmental conditions, and Physiological performed
 1349 separately by morpho-functional groups and genus. Estimated regression coefficients include
 1350 degrees of freedom for the error (DFE), root-mean-square error (RMSE), coefficients of
 1351 determination (R^2) and the adjusted R^2 statistics, Mallows' Cp criterion (Cp), Akaike Information
 1352 Criterion (AIC), Bayesian Information Criterion (BIC) minimum, F Ratio test, and p-value for the
 1353 test (Prob > F). Model information includes value of the constant a ($\delta^{13}\text{C}$, ‰), standard error (SE),
 1354 t ratio and Prob > |t| (values * are significant).

Full model	Estimated regression coefficients								Model constant (a)				
	DFE	RMSE	R^2	Adjust R^2	Cp	AICc	BIC	F ratio	Prob > F	$\delta^{13}\text{C}$ (‰)	SE	t ratio	Prob > t
Coastline sector + Habitats features + Morphofunctional group													
I-Morpho-functional	593	2.79	0.60	0.46	216	4,301	5,160	20.8	<.0001*	-13.49	0.57	-23.52	<.0001*
Coastline sector + Environmental conditions + Morphofunctional group													
II-Morpho-functional	680	2.90	0.51	0.42	129	4,189	4,750	25.1	<.0001*	-13.42	0.54	-24.74	<.0001*
Coastline sector + Habitat features+ Genus													
I-Genus	482	2.66	0.71	0.51	327	4,565	5,655	15.8	<.0001*	-16.93	0.73	-23.27	<.0001*
Coastline sector + Environmental conditions + Genus													
II-Genus	494	2.49	0.72	0.55	310	4,374	5,438	14.8	0.0001*	-13.55	0.64	-21.17	<.0001*

1355

1356 Table 8. Constant of fitted regression model explaining the $\delta^{13}\text{C}$ variability by morpho-functional
 1357 groups. Model information includes value of the constant a ($\delta^{13}\text{C}$, ‰), standard error (SE), t ratio
 1358 and Prob > |t|. Only morpho-functional groups with significant effects are enlisted.

Term	Estimated	SE	Razón t	Prob > t
Model constant	-14.2	0.4	-40.80	<.0001**
R-Smaller-sized articulated corallines	4.5	1.7	2.58	0.0100*
O-Compressed with branched or divided thallus	1.2	0.5	2.66	0.0079*
C-Erect thallus	1.8	0.6	2.84	0.0046*
R-Larger-sized articulated corallines	6.3	0.8	7.95	<.0001*
O-Hollow with spherical or subspherical shape	5.0	0.5	10.51	<.0001*
R-Blade-like with one of few layers of cells	-5.9	3.0	-1.98	0.0476*
C-Tubular	-1.6	0.5	-3.26	0.0012**
R-Filamentous uni&pluriseriate with erect thallus	-2.2	0.6	-3.92	<.0001*
R-Flattened macrophytes with cortication	-8.9	1.3	-7.10	<.0001*

1359 *p<0.05, **p<0.0001

1360

1361

1362

1363

1364

1365

1366

1367

1368 Table 9. Constant of fitted regression model explaining the $\delta^{13}\text{C}$ variability by genus. Model
 1369 information includes value of the constant a ($\delta^{13}\text{C}$, ‰), standard error (SE), t ratio and Prob > |t|.
 1370 Only genus with significant effects are enlisted.

Term	$\delta^{13}\text{C}$, ‰ estimated	SE	t value	Prob > t
Model constant	-14.7	0.2	-62.64	<.0001**
<i>Amphiroa</i>	6.8	0.8	9.05	<.0001**
<i>Codium</i>	2.3	0.6	4.08	<.0001**
<i>Colpomenia</i>	5.4	0.4	14.02	<.0001*
<i>Corallina</i>	6.4	2.9	2.22	0.0269*
<i>Gracilaria</i>	-0.9	0.4	-2.18	0.0294*
<i>Hydroclathrus</i>	7.3	1.1	6.59	<.0001**
<i>Jania</i>	5	1.7	2.97	0.0031*
<i>Padina</i>	2.2	0.5	4.8	<.0001**
<i>Polysiphonia</i>	-3.7	0.8	-4.82	<.0001**
<i>Schizymenia</i>	-19.1	2.1	-9.33	<.0001**
<i>Spyridia</i>	-1.5	0.7	-2.10	0.0361*
<i>Struveopsis</i>	4.1	1.3	3.15	0.0017*
<i>Tacanoosca</i>	3.5	1.3	2.71	0.0070*

1371 *p<0.05, **p<0.001

1372

1373

1374 Table 10. Constant of fitted regression model explaining the $\delta^{13}\text{C}$ variability by species. Model
 1375 information includes value of the constant a ($\delta^{13}\text{C}$, ‰), standard error (SE), t ratio and Prob > |t|.
 1376 Only genus with significant effects are enlisted.

Term	$\delta^{13}\text{C}$, ‰ estimated	SE	t value	Prob > t
Model constant	-14.6	0.2	-93.22	<.0001**
<i>Amphiroa misakiensis</i>	7.1	2.8	2.55	0.0110*
<i>Amphiroa</i> sp.	8.1	0.9	8.67	<.0001**
<i>Amphiroa</i> sp.2	6.6	1.6	4.1	<.0001**
<i>Amphiroa</i> sp.3	8.2	2.8	2.95	0.0033**
<i>Caulerpa peltata</i>	3.9	1.6	2.4	0.0165*
<i>Cladophora microcladioides</i>	-7.2	2	-3.64	0.0003**
<i>Codium brandegeei</i>	2.8	1.1	2.63	0.0088**
<i>Codium simulans</i>	3.2	0.9	3.41	0.0007**
<i>Codium</i> sp.	3	1.3	2.4	0.0167*
<i>Colpomenia ramosa</i>	3.2	1.4	2.27	0.0237*
<i>Colpomenia sinuosa</i>	4.4	1.1	4.17	<.0001**
<i>Colpomenia</i> sp.	3.6	0.9	4.27	<.0001**
<i>Colpomenia tuberculata</i>	5.9	0.4	15.45	<.0001**
<i>Corallina vancouverensis</i>	6.3	2.8	2.27	0.0238*
<i>Grateloupia filicina</i>	-2.4	1.1	-2.08	0.0382*
<i>Halymenia actinophysa</i>	-9.9	2.8	-3.57	0.0004**

<i>Hydroclathrus clathratus</i>	7.2	1.1	6.82	<.0001**
<i>Hypnea johnstonii</i>	3.4	1.3	2.74	0.0063**
<i>Hypnea pannosa</i>	2.8	1.3	2.24	0.0256*
<i>Jania</i> sp.	5	2	2.56	0.0106*
<i>Padina durvillei</i>	1.4	0.5	2.87	0.0043**
<i>Padina</i> sp.	3.5	0.7	4.77	<.0001**
<i>Polysiphonia mollis</i>	-5.2	1.1	-4.93	<.0001**
<i>Polysiphonia</i> sp.	-4.8	1.4	-3.44	0.0006**
<i>Pyropia thuretii</i>	-5.5	2.8	-1.98	0.0480*
<i>Rhizoclonium riparium</i>	-5.1	1.6	-3.15	0.0017**
<i>Rhodymenia</i> sp.	-4.1	2	-2.08	0.0380*
<i>Schizymenia pacifica</i>	-19.2	2	-9.76	<.0001**
<i>Spyrida</i> sp.	-2.5	1.3	-1.97	0.0496*
<i>Struveopsis</i> sp.	4	1.4	2.86	0.0044**
<i>Tacanoosca uncinata</i>	3.4	1.3	2.74	0.0062**
<i>Ulva acanthophora</i>	-1.2	0.6	-2.06	0.0399*
<i>Ulva compressa</i>	-3.2	1.4	-2.33	0.0203*

1377
1378

*p<0.05, **p<0.001